Fictitious Fluid Approach and Anomalous Blow-up of the Dissipation Rate in a 2D Model of Concentrated Suspensions

Leonid Berlyand[1], Yuliya Gorb[2], and Alexei Novikov[3]

[1] Department of Mathematics & Materials Research Institute, Pennsylvania State University, McAllister Bld., University Park, PA 16802, USA, berlyand@math.psu.edu
[2] Department of Mathematics, Texas A&M University, College Station, TX 77843, USA, gorb@math.tamu.edu
[3] Department of Mathematics, Pennsylvania State University, University Park, PA 16802, USA, anovikov@math.psu.edu

Summary. We present a two-dimensional (2D) mathematical model of a highly concentrated suspension or a thin film of the rigid inclusions in an incompressible Newtonian fluid. Our objectives are two-fold: (*i*) to obtain all singular terms in the asymptotics of the effective viscous dissipation rate as the interparticle distance parameter δ tends to zero, (*ii*) to obtain a qualitative description of a microflow between neighboring inclusions in the suspension.

Due to reduced analytical and computational complexity, 2D models are often used for a description of 3D suspensions. Our analysis provides the limits of validity of 2D models for 3D problems and highlights novel features of 2D physical problems (e.g. thin films). It also shows that the Poiseuille type microflow contributes to a singular behavior of the dissipation rate. We present examples in which this flow results in anomalous rate of blow up of the dissipation rate in 2D. We show that this anomalous blow up has no analog in 3D.

While previously developed techniques allowed to derive and justify the leading singular term only for special symmetric boundary conditions, a *fictitious fluid approach*, developed in this paper, captures *all* singular terms in the asymptotics of the dissipation rate for generic boundary conditions. This approach seems to be an appropriate tool for rigorous analysis of 3D models of suspensions as well as various other models of highly packed composites.

Key words: concentrated suspensions, effective viscous dissipation rate, Stokes flow, discrete network approximation, variational bounds, Poiseuille flow.

1 Introduction

Many classical and novel engineering processes involving multiphase flow require to capture the effective behavior of suspensions. The problem of the behavior of suspensions is important in geophysics (mud-flow and debris flow rheology), pharmacology (drugs design), ceramics processing among others. Wide range of experimental (see, e.g., [1, 3, 4, 21, 34, 40, 46–48, 54]), and numerical (see, e.g., [17, 38, 42, 51, 56, 58]) results are available.

We consider a 2D mathematical model of a non-colloidal (Browning motion can be neglected) concentrated suspension of neutrally buoyant rigid particles (inclusions) in a Newtonian fluid. The suspension occupies a 2D domain Ω, and rigid inclusions are modeled by disks of equal radii, which do not touch. The main objective is to characterize in a rigorous mathematical framework the dependence of the effective rate of the dissipation of the viscous energy (effective viscous dissipation rate) of such a suspension on the geometry of inclusions array and applied boundary conditions on $\partial\Omega$. We focus on densely packed suspensions when the concentration of inclusions is close to maximal, which means that the distance between neighboring inclusions (*interparticle distance*) is much smaller than their sizes. We consider an irregular (non-periodic) array of disks and our analysis takes into account the variable distances between adjacent inclusions.

Our initial interest in study highly concentrated suspensions was motivated by the problem of sedimentation in suspensions of rigid particles in a viscous fluid. In this problem a number of phenomena is not well-understood, e.g. speed-up of sedimentation by the applied shearing as it occurs in dewatering of the waste water sludge in a centrifuge [30, 55]. Often 2D mathematical models are used in study of suspensions (e.g. [20, 22, 23, 30, 32, 33, 37, 49, 53, 60]). Then the issue of validity of conclusions obtained by analysis of 2D models for actual 3D physical problems becomes crucial. The surprising result of this work is that 2D model possesses features that are not seen in 3D, and not only is analysis of 2D problem different but also physics is different. A possible application of the 2D model of suspensions is to describe biological thin films (so-called "bio-suspensions"), which have been recently produced by experimentalists (see e.g. [57, 61]), and are extensively studied now due to their application in pharmaceutical industry.

The main features of the problem under consideration are the high concentration of the inclusions and the irregular geometry of their spatial distribution. In this paper we focus on the effective rate of the dissipation of the viscous energy $\widehat{W} = \widehat{W}(\boldsymbol{u})$, where $\boldsymbol{u}$ is the velocity of the incompressible fluid (see the precise definition in Section 2). It is a primary quantity of interest in describing the effective rheological properties of suspensions such as effective viscosity (see e.g. [6, 7, 13, 24, 39, 52]).

For highly concentrated suspensions of rigid inclusions, the effective viscous dissipation rate $\widehat{W}$ exhibits a singular behavior (see e.g. [7, 13, 26, 29, 52, 56]) and its understanding is a fundamental issue. A formal asymptotic

analysis of the singular behavior of $\widehat{W}$ in a thin gap between a single pair of two closely spaced spherical inclusions in a Newtonian fluid was performed in [26]. In this work only translational motions of inclusions but not rotational were considered and the asymptotics of the form $C\delta^{-1} + O(\ln 1/\delta)$, where δ is the distance between two spheres, was obtained. Based on the analysis of a single pair of spheres the authors of [26] suggested that the asymptotics of the effective viscosity of the periodic array of inclusions is of the same form, that is, the main singular behavior is of $O(\delta^{-1})$. Next, a periodic array of inclusions in a Newtonian fluid was considered in [52]. Under the assumption that all inclusions follow the shear motion of the fluid (formula (5) in [52]) it was shown that $\widehat{W} = O(\delta^{-1})$. This assumption is analogous to the well-known Cauchy-Born hypothesis in solid state physics, which is known to be *not* always true [27]. Indeed, in the case of suspensions it was shown in [13] that for shear external boundary conditions the inclusions may not follow the shear motion. Moreover, it was shown in numerical studies of [56] that the asymptotics $O(\delta^{-1})$ may or may not hold for suspensions of a large number of inclusions with generic boundary conditions. There it was observed numerically that while in some cases the asymptotics of the effective viscosity is of order $1/\delta$, in other cases it is of order $\ln 1/\delta$. Also the problem of the exact analytical form of the singular behavior for generic suspensions was posed in [56] (p. 140) which motivated subsequent studies of [7, 13] and the present paper.

In [7] a formal asymptotic analysis of the effective viscosity in 3D for a disordered array of inclusions was performed. In a view of discrepancies between predictions of the formal asymptotic analysis [26] and numerics [56] such formal asymptotics requires a mathematical justification. In [7] for special (extensional) boundary conditions the leading term of the asymptotics of the effective viscosity as $\delta \to 0$, where δ is the characteristic spacing between neighboring inclusions, was justified in a 2D model. In subsequent work [13] this leading term, that exhibits a so-called *strong blow up* of order $\delta^{-3/2}$, was analyzed. It turned out that in many important cases, e.g. when shear boundary conditions are applied, this term degenerates, so the next term of order $\delta^{-1/2}$, that exhibits a so-called *weak blow up*, becomes the leading term of the asymptotics in many physical situations.

However, in [7] are only the strong blow up but not the other singular terms in the asymptotic expansion of the effective viscosity were captured and justified. In this paper we introduce a *fictitious fluid approach* which allows to derive the complete asymptotic description of the singularity of the effective viscous dissipation and justified it. In particular, we ruled out singular terms other than presented in Theorem 2.1. Previously [7, 8, 13, 26, 29, 52, 56] inclusions in a densely packed suspension were characterized by sets of their translational and rotational velocities, so-called discrete variables. Our analysis shows that in order to obtain the complete asymptotics of singular behavior it is necessary use an additional set of discrete variables, permeation constants, which, to the best of our knowledge, have not been used in previous studies of

concentrated suspensions. We now explain the physical consequences of this asymptotics.

The key feature of rheology of concentrated suspensions is that the dominant contribution to the effective viscous dissipation rate comes from thin gaps (lubrication regions) between closely spaced neighboring inclusions [45]. The mathematical techniques introduced in the above mentioned works [7, 26, 52] utilized this observation. More specifically, they took into account certain types of relative movements of inclusions which resulted in the corresponding microflows in the gaps. The formal asymptotics in [26] was based on analysis of the squeeze motion, when two inclusions move toward each other along the line joining their centers (see Fig. 2.7*c*) but did not provide the detailed analysis of other motions, which was sufficient for certain type of boundary conditions (e.g. extensional boundary conditions) but not sufficient for others. A justification of the formal asymptotics was not considered in [26] (see also [29] where similar results were obtained).

In [7] four types of relative motions of neighboring inclusions were considered which result in a singular behavior of dissipation rate: the squeeze (Fig. 2.7*c*), the shear (Fig. 2.7*b*) and two rotations (Fig. 2.8). While it was sufficient for the analysis of the leading term of the effective viscous dissipation rate (in a suspension of free particles) which was the goal of [7], in the present paper we observed that this analysis does not provide a complete picture of microflows. Indeed, the Poiseuille flow in 2D also contributes into the singular behavior. Examples in the present paper suggest that when an external field is applied to inclusions in a suspension, this Poiseuille flow may give rise to an anomalous strong rate of blow up (called a *superstrong blow up*, of order $\delta^{-5/2}$) of the viscous dissipation rate, whereas for suspensions of free inclusions there is at most strong blow up (of order $\delta^{-3/2}$). Furthermore, the complete asymptotic description of the singular behavior of the viscous dissipation rate obtained in this paper leads to the complete description of microflows in the gaps between neighboring inclusions (Fig. 2.7-2.10).

The techniques of [7, 13] and the present paper are based on the *discrete network approximation*. Discrete networks have been used as analogies of the continuum problems in various areas of physics and engineering for a long time (see, for example, [11] and references therein, and see also the recent review [50] for various applications of networks in social and biological studies). However, the fundamental issue of relationship between a continuum problem and the corresponding discrete network was not addressed.

We briefly outline here the development of the discrete network approximation for high contrast material.

The local formal asymptotic analysis for the effective conductivity of a *periodic array* of ideally conducting particles in a matrix of the finite conductivity was done in [39]. The key observation of [39] was that the dominant contribution to the asymptotics of the effective conductivity comes from thin gaps between neighboring inclusions so that flows outside gaps are negligible of those in gaps. Asymptotic formula for the electric field in such gaps

obtained in [39] was later used for global analysis of effective properties in [9, 11, 12, 14, 16] even for non-periodic composites.

In [41] fundamental ideas of the method of geometric averaging were introduced. In particular, for a high contrast medium described by the periodic function

$$e^{\lambda S(\boldsymbol{x})},\ \lambda \gg 1, \tag{1.1}$$

with a smooth phase function $S(\boldsymbol{x})$, it was shown that there is a strong channeling of the flow at the saddle points of $S(\boldsymbol{x})$. Hence, the effective properties of high contrast media depend crucially on its geometric characterization. Namely, for the medium (1.1) they are essentially determined by two factors: *(i)* the location of saddle points of the phase function $S(\boldsymbol{x})$ (geometry) and *(ii)* asymptotics as $\lambda \to \infty$.

The next major step in study of overall properties of high contrast materials was done in [14–16] by introducing novel ideas in the geometrical averaging method. These studies pioneered the idea of the *discrete network approximation* for high contrast continuum media. In particular, in [16] the principal issue of the relationship between the continuum and discrete models was addressed using rigorous asymptotic analysis.

In [16] the construction of the network was done for the function (1.1). The effective resistivity was obtained in terms of the principal curvatures κ^+, κ^- of the function $S(\boldsymbol{x})$ at the saddle points of $S(\boldsymbol{x})$. The direct and dual variational principles were used there to rigorously justify the discrete network approximation by constructing matching up to the leading term bounds for asymtotics of the effective resistivity. These bounds are given by discrete variational principles that can be interpreted in terms of networks. The key step in this duality approach is the construction of test functions. There is no general recipe for construction of such functions. Therefore, implementation of this approach is a highly nontrivial analysis problem since a test function which will work for one problem may not work for another. Indeed, these functions essentially depend on physical and geometrical features of the problem. In particular, in [16] an original construction of test function for the Kozlov-type medium (1.1) was developed.

Results of [16] have been applied to the inverse problem of the recovery of the conductivity from the boundary measurements, when there are regions of high contrast in the medium such that standard approximation methods (Born approximation) do not work. It has been shown in [15] that imaging of the conductivity of such a medium is asymptotically equivalent to the identification of a resistor network from voltage and current measurements at the boundary vertices. Techniques of [16] have also been generalized for the problem of quasi-static transport in high contrast conductive media [14].

Subsequently, the discrete network approximation for a medium with piecewise constant characteristics, which correspond to particle-filled (particulate) composites, was developed for a scalar conductivity problem in [9, 11, 12]. Since the phase-function $S(x)$ is not smooth for such medium the building

block of this network is the Keller's solution [39] (for conductivity in a gap between closely placed inclusions) in place of the Kozlov's solution [41] (which is the building block of the network in [14–16]). Also for this class of problems the high-constrast parameter $\varepsilon = 0$, and asymptotic analysis is performed as the interparticle distance parameter $\delta \to 0$.

In [11] the following fundamental issue has been raised. Is it possible that the rate of the overall properties (e.g., effective conductivity) differs by an order of magnitude from the blow-up of local properties (e.g., conductivity in a single gap)? For the scalar conductivity problem it was shown in [11] that the answer is negative. However, for an analogous vectorial problem of effective rate of viscous dissipation rate [7, 13] the answer is positive. This provides an explanation for a partial disagreement between numerical results [56] for suspensions; and earlier theoretical predictions based on asymptotics for a single pair of inclusions [26].

The latter observation led to the conclusion that the leading asymptotic term may not characterize the effective viscosity of suspensions, due to its possible degeneracy. Hence evaluation of the effective viscosity requires calculation of *all singular terms* in its asymptotic expansion. This was the original motivation of the present work. The key technical step in obtaining this asymptotics is a delicate construction of test functions for the direct and dual variational principles. The *fictitious fluid approach*, developed in this paper, allows for such a construction. The asymptotic formula with all singular terms results in a *complete* description of microflows in suspensions, as oppose to the partial description of the microflow in [7, 26, 29, 52].

The techniques in [9, 11, 12] for scalar problems in both 2D and 3D were based on a direct (one-step) discretization of the original continuum problem. The straightforward extension of these techniques to a vectorial problem of effective viscosity is not possible, due to the global divergence free condition. The first construction of divergence-free vectorial test functions was developed in [7]. This construction was based on the direct discretization and, in particular, it captured long-range hydrodynamic interactions and revealed the global nature of the divergence free condition (all particles are taken into account). In [7] the leading term of the asymptotics for the extensional viscosity (strong blow up) was obtained and justified. However, it was not possible to find the shear viscosity (weak blow up) within the framework of one-step discretization. This motivated the introduction of our two-step discretization based on the fictitious fluid approach.

We briefly describe now the idea behind this approach. As mentioned before, it consists of two steps. In step 1 we introduce a fictitious fluid domain which comprises thin gaps between neighboring inclusions. The dissipation rate restricted to this domain is denoted by $\widehat{W}_{\boldsymbol{\Pi}}$. We show that for generic Dirichlet boundary conditions it describes the singular behavior in the following sense:

$$\widehat{W} = \widehat{W}_{\boldsymbol{\Pi}} + h.o.t. \quad \text{as} \quad \delta \to 0.$$

In step 2 we perform a discretization of $\widehat{W}_{\boldsymbol{\Pi}}$, that is, the continuum problem for $\widehat{W}_{\boldsymbol{\Pi}}$ is reduced to an algebraic problem on a graph, called a *network problem*. By using the fictitious fluid approach in this step most of the difficulties due to global constraints are eliminated. Namely, it allows to construct the lower variational bound matching up to *all* singular terms with the upper bound. Recall that in [7] the main difficulty came from extending test functions outside the necks, while the fictitious fluid approach gets rid of this issue completely, hence, making analysis much easier and more successful in sense of capturing all singular terms of asymptotics of the dissipation rate.

The network problem is a minimization of a quadratic form whose coefficients depend on R, μ and boundary data. The quadratic form on the minimizing set of discrete variables is called the *discrete viscous dissipation rate* and denoted by $\mathcal{I}$. Unknowns of this problem are vectors $\mathbb{U} = \{\boldsymbol{U}^i\}_{i=1}^N$, $\boldsymbol{\omega} = \{\omega^i\}_{i=1}^N$, the translational and angular velocities of inclusions, respectively, and a collection of numbers $\boldsymbol{\beta} = \{\beta_{ij}\}$ characterizing the Poiseuille microflow between a pair of inclusions and called permeation constants. The discrete dissipation rate $\mathcal{I}$ is given by:

$$\mathcal{I} = \mathcal{I}_1(\boldsymbol{\beta})\delta^{-5/2} + \mathcal{I}_2(\mathbb{U}, \boldsymbol{\omega}, \boldsymbol{\beta})\delta^{-3/2} + \mathcal{I}_3(\mathbb{U}, \boldsymbol{\omega}, \boldsymbol{\beta})\delta^{-1/2}, \text{ as } \delta \to 0 \qquad (1.2)$$

where $\mathcal{I}_k$, $k = 1, 2, 3$, are explicitly computable quadratic polynomials of $\mathbb{U}$, $\boldsymbol{\omega}$, $\boldsymbol{\beta}$.

So the reduction of the problem to the problem in necks only reveals the significance of new set of discrete parameters $\boldsymbol{\beta}$ describing the Poiseuille microflow in gaps between neighbors. The contribution of this flow into singularity of viscous dissipation is large and has to be taken into account for complete asymptotic description of its singular behavior.

As a result we obtain the following asymptotic formula for the generic Dirichlet boundary conditions:

$$\frac{|\widehat{W} - \mathcal{I}|}{\mathcal{I}} = O(\delta^{1/2}) \quad \text{as} \quad \delta \to 0.$$

In fact, we prove the following result about the error term:

$$|\widehat{W} - \mathcal{I}| \leq \mu \left(\sum_{i,j} \mathbb{E}_1(\beta_{ij}) + \mathbb{E}_2(\boldsymbol{U}^i - \boldsymbol{U}^j) + \mathbb{E}_3(\omega^i) \right)$$

where $\mathbb{E}_1$, $\mathbb{E}_2$, $\mathbb{E}_3$ are quadratic polynomials of β_{ij}, difference $\boldsymbol{U}^i - \boldsymbol{U}^j$ and ω^i, respectively, whose coefficients are independent of δ.

Finally, we analyze the physical ramification of the obtained asymptotic formula by presenting several examples. We construct an a example of a suspension in a strong "pinning" external field, where $\widehat{W}$ is of order $\delta^{-5/2}$ (superstrong blow up). We also show an example of the superstrong blow up due to the boundary layer effect. Note that to the best of our knowledge this rate of

blow up was not observed before and we call it an *anomalous rate*. For generic suspensions (free particles or a weak external field) we expect that $\boldsymbol{\beta} = O(\delta)$ and, therefore, the first and the third terms of (1.2) are of the same order $O(\delta^{-1/2})$. For a hexagonal array of inclusions we prove that $\widehat{W}$ exhibits the strong blow up (of order $\delta^{-3/2}$) and $\boldsymbol{\beta} = \mathbf{0}$. Note that a typical close packing array in 2D is "approximately" hexagonal.

The paper is organized as follows. In Section 2 we give a mathematical formulation of the problem (Subsection 2.1), describe the fictitious fluid approach, and present our main results in Theorems 2.1, 2.2 (Subsection 2.2). In Subsection 2.3 we construct our discrete network and discuss how local flows in thin gaps between neighbors (microflows) contribute the effective viscous dissipation rate and state the theorem about a representation of the error term of the discrete approximation. In Section 3 we discuss main and present examples. Section 4 is devoted to the the fictitious fluid problem. In Section 5 we present results related to our discrete network. Conclusions are presented in Section 6. The coefficients of the quadratic form derived in Section 2 are given in Appendix.

Acknowledgments

The authors thank A.G. Kolpakov and A. Panchenko for careful reading of the manuscript and useful suggestions. The work of L. Berlyand was supported by NSF Grant No. DMS-0204637. The work of A. Novikov was supported by grants BSF-2005133 and DMS-0604600.

2 Formulation of the Problem and Main Results

2.1 Mathematical Formulation of the Problem

Consider an irregular or non-periodic array of N identical circular disks B^i, of the radius R distributed in a rectangular domain Ω. Denote by $\Omega_F = \Omega \backslash \bigcup_{i=1}^{N} B^i$ the *fluid domain* which is occupied by incompressible fluid with viscosity μ (see Fig. 2.1). Disks B^i represent absolutely rigid inclusions. Inertia of both fluid and inclusions is neglected. In the fluid domain Ω_F consider the following boundary value problem:

$$
\begin{aligned}
&(a)\ \mu\triangle \boldsymbol{u} = \nabla p, && \boldsymbol{x}\in\Omega_F\\
&(b)\ \nabla\cdot\boldsymbol{u} = 0, && \boldsymbol{x}\in\Omega_F\\
&(c)\ \boldsymbol{u} = \boldsymbol{U}^i + R\omega^i(n_1^i\boldsymbol{e}_2 - n_2^i\boldsymbol{e}_1), && \boldsymbol{x}\in\partial B^i,\quad i=1\dots N\\
&(d)\ \int_{\partial B^i}\boldsymbol{\sigma}(\boldsymbol{u})\boldsymbol{n}^i ds = \boldsymbol{0} && i=1\dots N\\
&(e)\ \int_{\partial B^i}\boldsymbol{n}^i\times\boldsymbol{\sigma}(\boldsymbol{u})\boldsymbol{n}^i ds = 0, && i=1\dots N\\
&(f)\ \boldsymbol{u} = \boldsymbol{f}, && \boldsymbol{x}\in\partial\Omega
\end{aligned}
\tag{2.1}
$$

where $\boldsymbol{u}(\boldsymbol{x})$ is the velocity field at a point $\boldsymbol{x}\in\Omega_F$, $p(\boldsymbol{x})$ is the pressure, $\boldsymbol{\sigma}(\boldsymbol{u}) = 2\mu\boldsymbol{D}(\boldsymbol{u}) - p\boldsymbol{I}$ is the stress tensor, $D_{ij}(\boldsymbol{u}) = \dfrac{1}{2}\left(\dfrac{\partial u_i}{\partial x_j} + \dfrac{\partial u_j}{\partial x_i}\right)$, $i,j=1,2$, is the rate of strain which satisfies the incompressibility condition: $\operatorname{tr}\boldsymbol{D}(\boldsymbol{u}) = 0$, another form of (2.1$b$). The vector $\boldsymbol{n}^i = (n_1^i, n_2^i)$ is the outer normal to B^i. Constant vectors $\boldsymbol{U}^i = (U_1^i, U_2^i)$ and scalars ω^i, $i=1,\dots,N$, which are translational and angular velocities of the inclusion B^i, respectively, are to be found in the course of solving the problem.

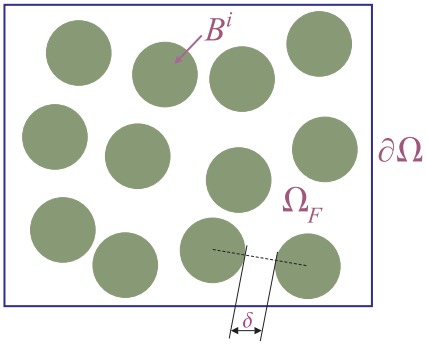

Fig. 2.1. Domain Ω_F occupied by the fluid of viscosity μ, and disordered array of closely spaced inclusions B^i

Here N is closed to maximal packing number $N_{max} = N_{max}(\Omega, R)$. This number is finite and $|N - N_{max}|$ depends on the small parameter δ called interpaticle distance.

We consider the linear external boundary conditions of the form:

$$
\boldsymbol{f} = A\boldsymbol{x} = \begin{pmatrix} a & b\\ c & -a\end{pmatrix}\begin{pmatrix} x\\ y\end{pmatrix},\quad \boldsymbol{x}\in\partial\Omega,
\tag{2.2}
$$

where the components a, b, c of the matrix A are given constants. Note that the most general form of the linear boundary conditions is $\boldsymbol{f} = \boldsymbol{f}_0 + A\boldsymbol{x}$ where $\boldsymbol{f}_0$ is a constant vector and $\boldsymbol{x}\in\partial\Omega$. Observe that when $a = 0$ and

$b = -1/c$ the vector $A\boldsymbol{x}$ corresponds to a rotation and $\boldsymbol{f}_0$ to a translation of the boundary, hence, $\boldsymbol{f}$ describes the rigid body motion of $\partial\Omega$. Hereafter, we exclude this trivial motion from our consideration assuming that $a = 0$ and $b = -1/c$ does not hold simultaneously in (2.2) and $\boldsymbol{f}_0 = \boldsymbol{0}$. We use such boundary conditions for two reasons: a) for technical simplicity, which does not lead to the loss of generality; b) they include the *shear* (when $a = c = 0$, $b = 1$) and *extensional* ($a = 1$, $b = c = 0$) boundary conditions (see e.g. [13]) which model two basic types of viscometric measurements (see Fig. 2.2). It is possible to extend our results to arbitrary Dirichlet boundary conditions $\boldsymbol{f} \in H^{1/2}(\partial\Omega)$ satisfying $\displaystyle\int_{\partial\Omega} \boldsymbol{f} \cdot \boldsymbol{n} ds = 0$.

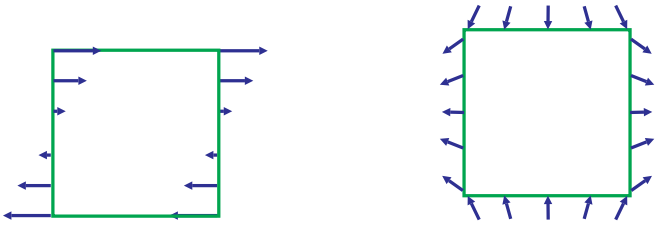

(a) shear (b) extensional

Fig. 2.2. Shear and extensional external boundary conditions

For an arbitrary set $A \subseteq \Omega_F$ consider the following integral:

$$\begin{aligned} W_A(\boldsymbol{v}) &= \frac{1}{2}\int_A \boldsymbol{\sigma}(\boldsymbol{v}) : \boldsymbol{D}(\boldsymbol{v}) = \mu \int_A \boldsymbol{D}(\boldsymbol{v}) : \boldsymbol{D}(\boldsymbol{v}) d\boldsymbol{x} \\ &= \mu \int_A \left[\left(\frac{\partial v_1}{\partial x}\right)^2 + \frac{1}{2}\left(\frac{\partial v_1}{\partial y} + \frac{\partial v_2}{\partial x}\right)^2 + \left(\frac{\partial v_2}{\partial y}\right)^2 \right] d\boldsymbol{x} \end{aligned} \tag{2.3}$$

where $\boldsymbol{v} = (v_1, v_2)$. Then the variational formulation of (2.1) is:

$$\text{Find} \quad \boldsymbol{u} \in V, \quad \text{such that } W_{\Omega_F}(\boldsymbol{u}) = \min_{\boldsymbol{v} \in V} W_{\Omega_F}(\boldsymbol{v}), \tag{2.4}$$

where the set V of admissible vector fields is defined by

$$\begin{aligned} V = \big\{ &\boldsymbol{v} \in \boldsymbol{H}^1(\Omega_F) : \ \nabla \cdot \boldsymbol{v} = 0 \text{ in } \Omega_F, \ \boldsymbol{v} = \boldsymbol{f} \text{ on } \partial\Omega, \\ &\boldsymbol{v} = \boldsymbol{U}^i + \boldsymbol{\omega}^i \times (\boldsymbol{x} - \boldsymbol{x}^i). \ \boldsymbol{x} \in \partial B^i, \quad i = 1, \ldots, N \big\}. \end{aligned} \tag{2.5}$$

$W_{\Omega_F}(\boldsymbol{u})$ is called the (continuum) viscous dissipation rate [44] and it is the principal quantity of interest in the study of effective properties of suspensions. We will use the following notation:

$$\widehat{W} := W_{\Omega_F}(\boldsymbol{u}). \tag{2.6}$$

The key feature of our problem is that we study suspensions where concentration of inclusions is close to its maximum. Therefore, the domain Ω_F depends on the characteristic interparticle distance parameter δ. Our main objective is to derive and justify an asymptotics of $\widehat{W}$ as $\delta \to 0$. We will show that the coefficients of this asymptotic formula are determined by the solution to a discrete network problem, which determine the discrete viscous dissipation rate.

2.2 The Fictitious Fluid Approach and Discretization

Note that using the notion of Voronoi tessellation we can decompose the domain Ω_F into *necks* $\boldsymbol{\Pi}$ and *triangles* $\boldsymbol{\Delta}$: $\Omega_F = \boldsymbol{\Pi} \cup \boldsymbol{\Delta}$ as in Fig. 2.4 (see Appendix B.1 of [10]). Necks connect either two disks (Fig. 2.3*a*) or a disk and a part of the boundary $\partial\Omega$ called a *quasidisk* (see Fig. 2.3*b*), that is, necks connect *neighbors*. The velocities of quasidisks are given by the prescribed boundary conditions (2.2). Note that near the boundary when quasidisks are involved the "triangles" are actually trapezoids. With slight abuse of terminology, we also call them *triangles*.

We distinguish boundary disks (quasidisks) and interior disks and introduce two sets of the corresponding indices. For indices of interior disks we use the notation $\mathbb{I} = \{1, \dots, N\}$. If the disk B^i centered at $\boldsymbol{x}_i$ is a quasidisk then i belongs to the set $\mathbb{B}$ of the indices of quasidisks. Also denote by $\mathcal{N}_i$ the set of indices of all neighbors of B^i.

For a given array of the disks and quasidisks B^i centered at $\boldsymbol{x}_i$, the ***discrete network*** is the graph $\mathcal{G} = (\mathcal{X}, \mathcal{E})$, with set of vertices $\mathcal{X} = \{\boldsymbol{x}_i : i \in \mathbb{I} \cup \mathbb{B}\}$ and set of edges $\mathcal{E} = \{e_{ij} : i \in \mathbb{I},\, j \in \mathcal{N}_i\}$ with e_{ij} connecting neighbors B^i and B^j.

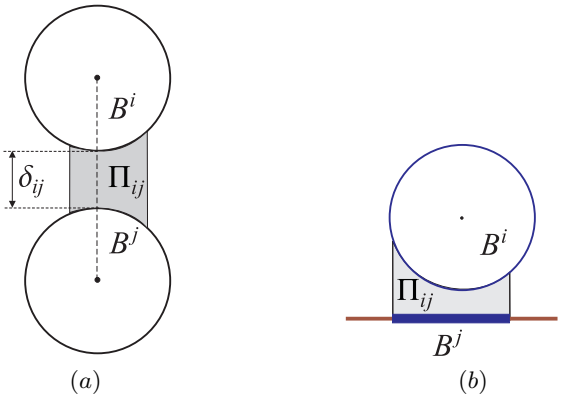

Fig. 2.3. (*a*) neck connecting two disks; (*b*) neck connecting disk B^i and quasidisk B^j

As mentioned in Introduction our main approach in study of the asymptotics of $\widehat{W}$ as $\delta \to 0$ consists of two steps. This two-step approach allows to separate geometric construction of the network and its subsequent asymptotic analysis.

In the first step, we show that the minimization problem (2.4) in the fluid domain Ω_F can be approximated by a "fictitious fluid" problem in which fluid is assumed to occupy necks $\boldsymbol{\Pi} = \bigcup_{i\in\mathbb{I}, j\in\mathcal{N}_i} \Pi_{ij}$ between closely spaced neighboring inclusions (the shadowed region in Fig. 2.4). We call $\boldsymbol{\Pi}$ the *fictitious fluid domain*. This reflects a well-known physical fact that for densely packed suspensions the dominant contribution to the viscous dissipation rate over the fluid domain comes from those necks. On the boundary of the complementary part of the domain (triangles in Fig. 2.4) the relaxed incompressibility conditions:

$$\int_{\partial\triangle_{ijk}} \boldsymbol{v}\cdot\boldsymbol{n} ds = 0, \quad i \in \mathbb{I}, \quad j,k \in \mathcal{N}_i, \tag{2.7}$$

are imposed.

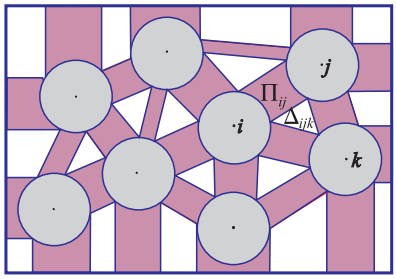

Fig. 2.4. The decomposition of the original fluid domain Ω_F into the fictitious fluid domain and the set of triangles

Below we show that the functional $W_{\Omega_F}(\cdot)$ given by (2.3) is decomposed as follows:

$$W_{\Omega_F}(\cdot) = W_{\boldsymbol{\Pi}}(\cdot) + W_{\boldsymbol{\Delta}}(\cdot) \quad \text{and} \quad \widehat{W} = \widehat{W}_{\boldsymbol{\Pi}} + \widehat{W}_{\boldsymbol{\Delta}}, \tag{2.8}$$

where $\widehat{W}_{\boldsymbol{\Pi}}$ is the effective viscous dissipation rate of the fictitious fluid defined below in (2.10) and $\widehat{W}_{\boldsymbol{\Delta}}$ is the remaining contribution from the domain $\boldsymbol{\Delta}$. Note that in (2.8) the "hat" quantities indicate the minimal values of the corresponding functionals.

Consider the problem of minimization of the functional $W_{\boldsymbol{\Pi}}$, defined by (2.3) over the fictitious fluid domain $\boldsymbol{\Pi}$, in the following class of functions:

$$V_{\boldsymbol{\Pi}} = \big\{\boldsymbol{v} \in \boldsymbol{H}^1(\boldsymbol{\Pi}) : \nabla \cdot \boldsymbol{v} = 0 \text{ in } \boldsymbol{\Pi},\ \int_{\partial \triangle_{ijk}} \boldsymbol{v} \cdot \boldsymbol{n} ds = 0 \text{ for all } \triangle_{ijk} \in \boldsymbol{\Delta},$$
$$\boldsymbol{v} = \boldsymbol{U}^i + R\omega^i(n_1^i \boldsymbol{e}_2 - n_2^i \boldsymbol{e}_1),\ \boldsymbol{x} \in \partial B^i,\ i = 1, \dots, N,\ \boldsymbol{v} = \boldsymbol{f} \text{ on } \partial\boldsymbol{\Pi} \cap \partial\Omega\big\}, \tag{2.9}$$

where $\boldsymbol{U}^i$ and ω^i, $i = 1, \dots, N$, are arbitrary constant vectors and arbitrary constants, respectively. The zero-flux condition through $\partial\triangle_{ijk}$ (2.7) is inherited from the problem in the original fluid domain Ω_F due to incompressibility condition of the fluid in triangles. Such a condition is a necessary (but not sufficient) for $\nabla \cdot \boldsymbol{v} = 0$ in the triangle $\triangle_{ijk}$.

We define the effective dissipation rate of the fictitious fluid by

$$\widehat{W}_{\boldsymbol{\Pi}} = \min_{\boldsymbol{v} \in V_{\boldsymbol{\Pi}}} W_{\boldsymbol{\Pi}}(\boldsymbol{v}). \tag{2.10}$$

The first principal result of this paper is that the dissipation rate $\widehat{W}$ can be approximated by the rate $\widehat{W}_{\boldsymbol{\Pi}}$ and $\widehat{W}_{\boldsymbol{\Delta}}$ can be neglected. To show this we need to introduce a small parameter of the problem, which is a characteristic interparticle distance δ.

For each pair of neighbors $\boldsymbol{x}_i$, $\boldsymbol{x}_j$ define

$$\delta_{ij} = \begin{cases} |\boldsymbol{x}_i - \boldsymbol{x}_j| - 2R, & \text{when } i, j \in \mathbb{I}, \\ |\boldsymbol{x}_i - \boldsymbol{x}_j| - R, & \text{when either } i \text{ or } j \in \mathbb{B}, \\ |\boldsymbol{x}_i - \boldsymbol{x}_j|, & \text{when } i, j \in \mathbb{B}. \end{cases} \tag{2.11}$$

As mentioned above, we study domains with closely spaced neighboring disks. More precisely, for all pairs of neighbors we assume that following *close-packing condition* holds.

Definition 1. *Write the minimal distance δ_{ij} (see Fig. 2.3) between any two neighboring disks B^i and B^j in the form $\delta_{ij} = \delta d_{ij}$, $0 < d_{ij} < R$. If the* ***characteristic interparticle distance*** *parameter δ is small, $\delta \ll 1$, then Ω_F is said to satisfy the* ***close-packing condition****.*

For technical simplicity we exclude the case of touching inclusions.

We remark that this definition describes uniformly dense arrays of disks. A more general definition which covers a notion of a "hole" corresponding to the void space in the composite is introduced and discussed e.g. in [9, 12].

Hereafter we call the array of inclusions under consideration a *quasi-hexagonal array* (e.g. in [12] it is referred to as "randomized hexagonal"). Recall, that for such arrays all neighbors are closely spaced and a typical number of nearest neighbors for a disk is six.

Hence, the mathematical thrust of step one of the fictitious fluid approach is in showing that the effective rate of the energy dissipation $\widehat{W}_{\boldsymbol{\Pi}}$ of the fictitious fluid captures the singular behavior of $\widehat{W}$, defined by (2.6), as $\delta \to 0$. More precisely, in Section 5 we prove the following theorem:

Theorem 2.1 (*Approximation by the fictitious fluid*). *Suppose an array of inclusions satisfies the close packing condition. Let $\widehat{W}$ be the effective viscous dissipation rate defined by* (2.5)-(2.6) *and $\widehat{W}_{\boldsymbol{\Pi}}$ be the viscous dissipation rate of the fictitious fluid defined by* (2.10)*. Then the following asymptotic formula holds:*

$$\frac{|\widehat{W}-\widehat{W}_{\boldsymbol{\Pi}}|}{\widehat{W}_{\boldsymbol{\Pi}}}=O(\delta^{1/2}) \quad \text{as } \delta\to 0. \tag{2.12}$$

In step two, we study asymptotics (blow up) of the effective viscous dissipation rate $\widehat{W}$ as $\delta\to 0$. In view of step one, this is reduced to finding of asymptotics of $\widehat{W}_{\boldsymbol{\Pi}}$. The latter is done by a construction of a discrete network approximation and introduction of a so-called discrete viscous dissipation rate $\mathcal{I}$. To show closeness of the continuum and the discrete dissipation rates, $\widehat{W}_{\boldsymbol{\Pi}}$ and $\mathcal{I}$, respectively, we employ the direct and dual variational techniques [7, 11, 12].

Also note that the conditions (2.1*d*,*e*) in the original problem led to significant technical difficulties in variational analysis of the effective viscous dissipation rate of [7], which is why the analysis of [7] is restricted to its leading singular term. In contrast, analogs of these conditions in the fictitious fluid problem are satisfied *automatically* by construction, which results in substantial simplification of the analysis and thus allows to capture all singular terms.

The approximation of the effective viscous dissipation rate $\widehat{W}$ by the discrete dissipation rate $\mathcal{I}$ is given by the following theorem.

Theorem 2.2 (*Approximation of the continuum dissipation rates by the discrete one*). *Suppose Ω_F satisfies the close packing condition and $\mathcal{I}=\min\limits_{(\mathbb{U},\boldsymbol{\omega},\boldsymbol{\beta})\in\boldsymbol{\mathcal{R}}} Q(\mathbb{U},\boldsymbol{\omega},\boldsymbol{\beta})$, where the positive definite quadratic form*

$$Q(\mathbb{U},\boldsymbol{\omega},\boldsymbol{\beta})=\mathcal{I}_1(\boldsymbol{\beta})\delta^{-5/2}+\mathcal{I}_2(\mathbb{U},\boldsymbol{\omega},\boldsymbol{\beta})\delta^{-3/2}+\mathcal{I}_3(\mathbb{U},\boldsymbol{\omega},\boldsymbol{\beta})\delta^{-1/2}$$

on the class of admissible discrete variables $(\mathbb{U},\boldsymbol{\omega},\boldsymbol{\beta})\in\boldsymbol{\mathcal{R}}$ defined in (2.33)-(2.37)*. Then the following approximation to the viscous dissipation rate holds:*

$$\frac{|\widehat{W}-\mathcal{I}|}{\mathcal{I}}=O(\delta^{1/2}) \quad \text{as } \delta\to 0, \tag{2.13}$$

Remark 2.1. $\mathcal{I}_i$ $(i=1,2,3)$ are explicitly computable quadratic polynomials of $(\mathbb{U},\boldsymbol{\omega},\boldsymbol{\beta})\in\boldsymbol{\mathcal{R}}$ from equations (2.36)-(2.37) below. These polynomials depend only on boundary data $\boldsymbol{f}$, viscosity μ and geometry of Ω_F.

The next subsection is devoted to the construction of these quadratic polynomials. We first introduce a set of discrete variables $(\mathbb{U},\boldsymbol{\omega},\boldsymbol{\beta})$, define a new variable β_{ij} in each neck Π_{ij} and explain how the quadratic form Q is obtained. We will also discuss the underlying structure of the flow in a neck (microflow) and physical ramifications of the obtained asymptotics (2.13) and (2.38) below.

2.3 Construction of the discrete network. Microflows.

(a) We begin with the discretization of the boundary conditions. Denote $\mathbb{U} = \{\boldsymbol{U}^i\}_{i\in\mathbb{I}\cup\mathbb{B}}$, $\boldsymbol{\omega} = \{\omega^i\}_{i\in\mathbb{I}\cup\mathbb{B}}$ where on the boundary $\partial\Omega$, that is, for $i \in \mathbb{B}$, these velocities are given by boundary conditions as follows:

$$\boldsymbol{U}^i = \begin{cases} \begin{pmatrix} ax \\ cx \end{pmatrix}, & \boldsymbol{x}_i \in \partial\Omega_{lat} \\ \\ \begin{pmatrix} by \\ -ay \end{pmatrix}, & \boldsymbol{x}_i \in \partial\Omega^{\pm} \end{cases} \quad \text{and } \omega^i = \begin{cases} c, & \boldsymbol{x}_i \in \partial\Omega^- \\ -c, & \boldsymbol{x}_i \in \partial\Omega^+ \\ b, & \boldsymbol{x}_i \in \partial\Omega^-_{lat} \\ -b, & \boldsymbol{x}_i \in \partial\Omega^+_{lat} \end{cases} \tag{2.14}$$

where $\boldsymbol{x}_i$ is the center of the quasidisk B^i and $\partial\Omega^+$ and $\partial\Omega^-$ are the upper and lower parts of $\partial\Omega$, respectively, and $\partial\Omega^-_{lat}$ and $\partial\Omega^+_{lat}$ are the lateral (left and right, respectively) boundary.

(b) Discretization of the incompressibility condition is implemented as follows. Decompose the domain Ω_F into curvilinear hexagons $\mathcal{A}_{ijk}$ as in Fig. 2.5:

$$\Omega_F = \bigcup_{i\in\mathbb{I},j,k\in\mathcal{N}_i} \mathcal{A}_{ijk}.$$

Each $\mathcal{A}_{ijk}$ consists of the line segments ℓ_{ij}, ℓ_{jk}, ℓ_{ki} (Fig. 2.5a) connecting

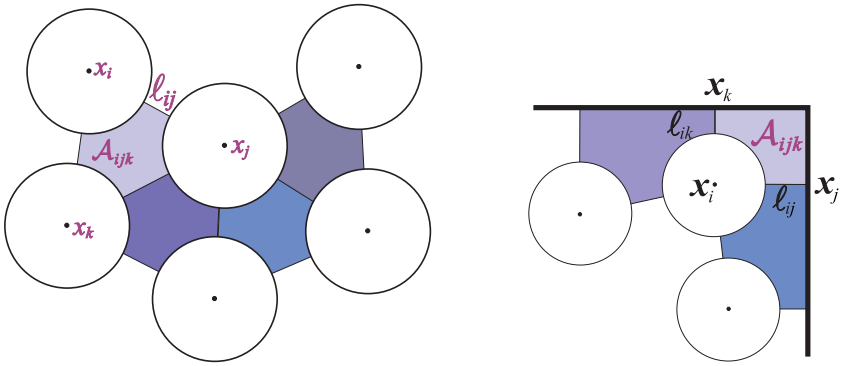

(a) (b)

Fig. 2.5. (a) Decomposition of Ω_F into curvilinear hexagons $\mathcal{A}_{ijk}$ and line ℓ_{ij} connecting neighbors B^i and B^j, (b) Construction of $\mathcal{A}_{ijk}$ at the corner of the boundary $\partial\Omega$

disks B^i, B^j, B^k and arcs a_i, a_j, a_k of the corresponding disk.[4] Then the weak incompressibility condition (2.7) for the class $V_{\boldsymbol{\Pi}}$ (2.9) becomes

[4] In the case when the disk B^i has two quasidisk neighbors B^j and B^k, that is, when B^k is in the corner as in Fig. 2.5b, then the domain $\mathcal{A}_{ijk}$ is actually a curvilinear pentagon. By slight abuse of terminology we still call it a "curvilinear hexagon".

$$\int_{\mathcal{A}_{ijk}} \boldsymbol{v}\cdot\boldsymbol{n}ds = 0, \quad \text{for any } \mathcal{A}_{ijk}, \quad i\in\mathbb{I}, j,k\in\mathcal{N}_i. \tag{2.15}$$

In order to continue our analysis at this point we must introduce a new set of discrete variables. Here we define permeation constants:

$$\begin{aligned}\beta^*_{ij} &= \frac{1}{R}\int_{\ell_{ij}} \boldsymbol{v}\cdot\boldsymbol{n}ds,\ i\in\mathbb{I},\ j\in\mathcal{N}_i,\\ \beta^*_{ij} &= \frac{1}{R}\int_{\ell_{ij}} \boldsymbol{f}\cdot\boldsymbol{n}ds,\ \ell_{ij}\subset\partial\Omega\,(i,j\in\mathbb{B}),\end{aligned} \tag{2.16}$$

where ℓ_{ij} is the line segment joining two neighbors B^i and B^j, $\boldsymbol{v}\in V_{\boldsymbol{\Pi}}$ and $\boldsymbol{n}$ is an outer normal to $\mathcal{A}_{ijk}$. Then (2.15) can be rewritten as:

$$\beta^*_{ij}+\beta^*_{jk}+\beta^*_{ki}+\frac{1}{R}\int_{a_i}\boldsymbol{U}^i\cdot\boldsymbol{n}^i ds+\frac{1}{R}\int_{a_j}\boldsymbol{U}^j\cdot\boldsymbol{n}^j ds+\frac{1}{R}\int_{a_k}\boldsymbol{U}^k\cdot\boldsymbol{n}^k ds=0,$$

for $i\in\mathbb{I}$, $j,k\in\mathcal{N}_i$ ($\boldsymbol{n}^i$ is a unit outer normal to ∂B^i), which can be further simplified as

$$\beta^*_{ij}+\beta^*_{jk}+\beta^*_{ki}+(\boldsymbol{U}^i+\boldsymbol{U}^j)\boldsymbol{p}^{ij}+(\boldsymbol{U}^j+\boldsymbol{U}^k)\boldsymbol{p}^{jk}+(\boldsymbol{U}^k+\boldsymbol{U}^i)\boldsymbol{p}^{ki}=0, \tag{2.17}$$

where vectors $\boldsymbol{q}^{ij}$ and $\boldsymbol{p}^{ij}$ are the unit vectors of the local system coordinate of two neighboring disks B^i and B^j as in Fig. 2.6. We call (2.17) the *weak incompressibility condition*. This formula explains the scaling $\frac{1}{R}$ in (2.16). In-

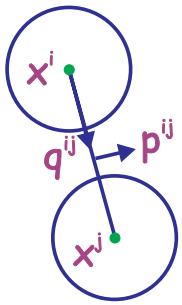

Fig. 2.6. Unit vectors of the local coordinate system

deed, from dimensional analysis $\int_{\ell_{ij}}\boldsymbol{v}\cdot\boldsymbol{n}ds$ must be divided by a characteristic lengthscale which is R in the curvilinear hexagonal $\mathcal{A}_{ijk}$.

(c) We finally discretize the Stokes equations in necks. This discretization is based on lubrication theory [2, 6, 45]. This theory describes thin film flows between two solid bodies sliding relative to each other. It is well-known (see e.g. [45]) that in dense suspensions the dominant hydrodynamic contribution to the viscous dissipation rate occurs in necks between closely spaced

inclusions, where lubrication equations are relevant. Lubrication theory determines fluid motion in such necks as a result of relative kinematic motion of the neighboring inclusions. This raises a question of the classification of *microflows*, that is, local flows in necks between two closely spaced neighbors.

Recall three classical types of microflows between two parallel plates: the shear, the squeeze, and the Poiseuille flow. The last one, however, is not related to motions of two plates relative one to another and therefore it is not described by lubrication theory. In this work we show that exactly these three types of microflows fully describe the motion of the fluid between two neighboring disks. Asymptotic analysis of microflows between two parallel plates technically is much simpler than that for inclusions with curvilinear boundaries, which is needed for suspensions.

As shown below, in classical 3D problem the Poiseuille microflow between two inclusions does not contribute to the singular behavior of the viscous dissipation rate. However, in analogous 2D problem (e.g. thin films) all three microflows are present and, moreover, the Poiseuille flow may result in anomalously strong singularity.

Thus, it is necessary to analyze kinematics of a pair of neighboring inclusions when one moves relative to the other. To this end for a pair of neighbors B^i and B^j, centered at $\boldsymbol{x}_i$ and $\boldsymbol{x}_j$, we choose the *local* coordinate system where the origin is at $(\boldsymbol{x}_i + \boldsymbol{x}_j)/2$ and the y-axis is directed along the vector connecting $\boldsymbol{x}_i$ and $\boldsymbol{x}_j$.

For clarity of presentation we consider two interior disks only (that is, $i \in \mathbb{I}$, $j \in \mathcal{N}_i \cap \mathbb{I}$). For an analogous construction in boundary necks ($i \in \mathbb{I}$, $j \in \mathcal{N}_i \cap \mathbb{B}$) see Appendix B.2 of [10].

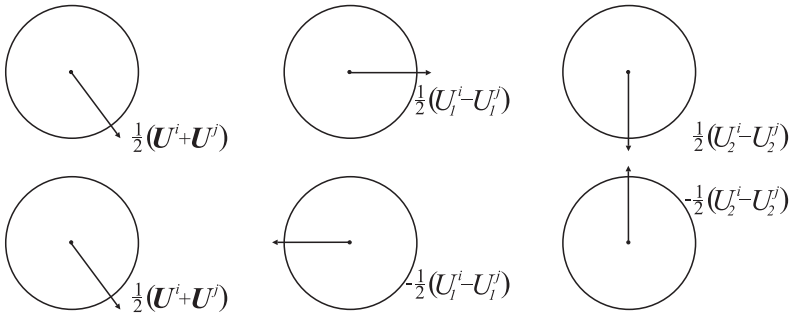

Fig. 2.7. Decomposition of translational velocities $\boldsymbol{U}^i$ and $\boldsymbol{U}^j$ into three elementary motions

There are exactly five elementary kinematic motions of inclusions. To see this we consider boundary conditions on ∂B^i, ∂B^j in (2.9) and first assume that $\omega^i = \omega^j = 0$. Then the conditions: $\boldsymbol{u} = \boldsymbol{U}^i$ on ∂B^i and $\boldsymbol{u} = \boldsymbol{U}^j$ on ∂B^j can be rewritten as follows:

$$\boldsymbol{u}|_{\partial B_i} = \frac{1}{2}(\boldsymbol{U}^i + \boldsymbol{U}^j) + \frac{1}{2}(U_1^i - U_1^j)\boldsymbol{e}_1 + \frac{1}{2}(U_2^i - U_2^j)\boldsymbol{e}_2,$$
$$\text{and } \boldsymbol{u}|_{\partial B^j} = \frac{1}{2}(\boldsymbol{U}^i + \boldsymbol{U}^j) - \frac{1}{2}(U_1^i - U_1^j)\boldsymbol{e}_1 - \frac{1}{2}(U_2^i - U_2^j)\boldsymbol{e}_2.$$

Hence, the translational velocities of disks are decomposed into three motions. First, when both inclusions and fluid move with the same velocity (see Fig. 2.7*a*), and therefore this motion does not contribute to the singular behavior of the viscous dissipation rate. Second, when one inclusion moves relative to the other producing the *shear* type motion (Fig. 2.7*b*) and, finally, the *squeeze* type motion (Fig. 2.7*c*) of the fluid.

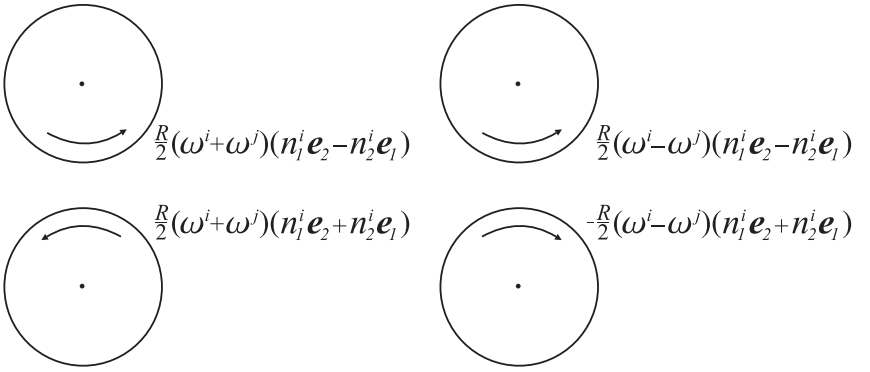

(*a*) rotation in the same direction

(*b*) rotation in the opposite directions

Fig. 2.8. Decomposition of the angular velocities ω^i and ω^j into two elementary motions

Similarly, assuming $\boldsymbol{U}^i = \boldsymbol{U}^j = \boldsymbol{0}$ in conditions on ∂B^i, ∂B^j in (2.9) we decompose them into two relative elementary motions: rotations of the disks in the same direction (Fig. 2.8*a*), and rotations of the disks in the opposite directions (Fig. 2.8*b*). Thus,

$$\boldsymbol{u}|_{\partial B_i} = \frac{R}{2}(\omega^i + \omega^j)(n_1^i\boldsymbol{e}_2 - n_2^i\boldsymbol{e}_1) + \frac{R}{2}(\omega^i - \omega^j)(n_1^i\boldsymbol{e}_2 - n_2^i\boldsymbol{e}_1)$$
$$\text{and } \boldsymbol{u}|_{\partial B^j} = \frac{R}{2}(\omega^i + \omega^j)(n_1^i\boldsymbol{e}_2 + n_2^i\boldsymbol{e}_1) + \frac{R}{2}(\omega^i - \omega^j)(-n_1^i\boldsymbol{e}_2 - n_2^i\boldsymbol{e}_1),$$

where $\boldsymbol{n}^i = (n_1^i, n_2^i)$ is the outer normal to ∂B^i.

Next consider microflows corresponding to the four kinematic motions contributing to the singular behavior of the dissipation rate described above. We further choose the microflow $\boldsymbol{u}_{lub}$ which minimizes the viscous dissipation rate in the neck Π_{ij} by imposing the natural boundary conditions on the lateral boundaries $\partial\Pi_{ij}^{\pm}$ (Fig. 2.9). That is, the function $\boldsymbol{u}_{lub}$ minimizes $W_{\Pi_{ij}}$ in the class:

$$\mathcal{V}_{ij} = \left\{ \boldsymbol{v} \in H^1(\Pi_{ij}) : \ \bigtriangledown \cdot \boldsymbol{v} = 0 \text{ in } \Pi_{ij}, \ \boldsymbol{v} = \boldsymbol{g}_i \text{ on } \partial B^i, \ \boldsymbol{v} = \boldsymbol{g}_j \text{ on } \partial B^j \right\} \tag{2.18}$$

$$\text{with } \ \boldsymbol{g}_i = \boldsymbol{U}^i + R\omega^i(n_1^i \boldsymbol{e}_2 - n_2^i \boldsymbol{e}_1), \quad \boldsymbol{g}_j = \boldsymbol{U}^j + R\omega^j(n_1^j \boldsymbol{e}_2 - n_2^j \boldsymbol{e}_1). \tag{2.19}$$

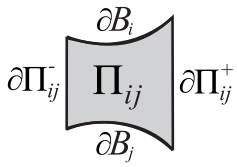

Fig. 2.9. Boundary of the neck Π_{ij}

Due to linearity the minimizer $\boldsymbol{u}_{lub}$ is decomposed into five vector fields corresponding to the relative motions of inclusions as in Fig. 2.7-2.8 as follows:

$$\begin{aligned} \boldsymbol{u}_{lub} = \frac{1}{2}(\boldsymbol{U}^i + \boldsymbol{U}^j) + [(\boldsymbol{U}^i - \boldsymbol{U}^j) \cdot \boldsymbol{p}^{ij}]\boldsymbol{u}_1 + [(\boldsymbol{U}^i - \boldsymbol{U}^j) \cdot \boldsymbol{q}^{ij}]\boldsymbol{u}_2 \\ + R(\omega^i + \omega^j)\boldsymbol{u}_3 + R(\omega^i - \omega^j)\boldsymbol{u}_4, \end{aligned} \tag{2.20}$$

where functions $\boldsymbol{u}_k$, $k = 1, \ldots, 4$ are minimizers of $W_{\Pi_{ij}}$ in $\mathcal{V}_{ij}$ (equation (2.18)) where boundary conditions (2.19) are replaced, respectively, by:
1) the *shear* motion of the fluid between two neighboring inclusions:

$$\boldsymbol{u}_1|_{\partial B^i} = \boldsymbol{g}_i = \frac{1}{2}\boldsymbol{e}_1, \quad \boldsymbol{u}_1|_{\partial B^j} = \boldsymbol{g}_j = -\frac{1}{2}\boldsymbol{e}_1, \tag{2.21}$$

2) the *squeeze* motion of the fluid between neighbors:

$$\boldsymbol{u}_2|_{\partial B^i} = \boldsymbol{g}_i = \frac{1}{2}\boldsymbol{e}_2, \quad \boldsymbol{u}_2|_{\partial B^j} = \boldsymbol{g}_j = -\frac{1}{2}\boldsymbol{e}_2, \tag{2.22}$$

3) the *rotation in the same directions*:

$$\boldsymbol{u}_3|_{\partial B^i} = \boldsymbol{g}_i = \frac{1}{2}(n_1^i \boldsymbol{e}_2 - n_2^i \boldsymbol{e}_1), \quad \boldsymbol{u}_3|_{\partial B^j} = \boldsymbol{g}_j = \frac{1}{2}(n_1^i \boldsymbol{e}_2 + n_2^i \boldsymbol{e}_1), \tag{2.23}$$

4) the *rotation in the opposite directions*:

$$\boldsymbol{u}_4|_{\partial B^i} = \boldsymbol{g}_i = \frac{1}{2}(n_1^i \boldsymbol{e}_2 - n_2^i \boldsymbol{e}_1), \quad \boldsymbol{u}_4|_{\partial B^j} = \boldsymbol{g}_j = -\frac{1}{2}(n_1^i \boldsymbol{e}_2 + n_2^i \boldsymbol{e}_1). \tag{2.24}$$

Let $\boldsymbol{u}$ be the minimizer of (2.4) then

$$\boldsymbol{u}_p := \boldsymbol{u} - \boldsymbol{u}_{lub} \tag{2.25}$$

minimizes $W_{\Pi_{ij}}$ in the class

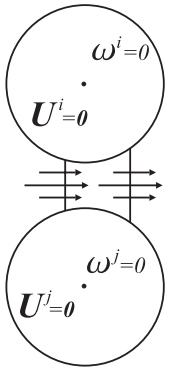

Fig. 2.10. The Poiseuille's microflow between motionless inclusions

$$\mathcal{V}_p = \Big\{ \boldsymbol{v} \in H^1(\Pi_{ij}) : \ \nabla \cdot \boldsymbol{v} = 0 \text{ in } \Pi_{ij}, \ \boldsymbol{v} = \boldsymbol{0} \text{ on } \partial B^i, \ \boldsymbol{v} = \boldsymbol{0} \text{ on } \partial B^j, \\ \frac{1}{R} \int_{\ell_{ij}} (\boldsymbol{v} + \boldsymbol{u}_{lub}) \cdot \boldsymbol{n} ds = \beta^*_{ij} \Big\}. \tag{2.26}$$

The vector field $\boldsymbol{u}_p$ describes the flow between two motionless inclusions, hence, it is natural to call it the *Poiseuille microflow*.

Denote by $\boldsymbol{\beta}^* = \{\beta^*_{ij}\}_{i \in \mathbb{I} \cup \mathbb{B}, j \in \mathcal{N}_i}$ and introduce the following set of discrete variables

$$\boldsymbol{\mathcal{R}}^* = \big\{ (\mathbb{U}, \boldsymbol{\omega}, \boldsymbol{\beta}^*) : \boldsymbol{U}^i, \omega^i \text{ satisfying (2.14) for } i \in \mathbb{B} \\ \text{and } (\mathbb{U}, \boldsymbol{\beta}^*) \text{ satisfying (2.17)} \big\}. \tag{2.27}$$

It is straightforward to show that (see Lemma 4.2)

$$\widehat{W}_{\boldsymbol{\Pi}} = \min_{(\mathbb{U}, \boldsymbol{\omega}, \boldsymbol{\beta}^*) \in \boldsymbol{\mathcal{R}}^*} \sum_{i \in \mathbb{I}, j \in \mathcal{N}_i} \min_{V_{ij}} W_{\Pi_{ij}}(\cdot), \tag{2.28}$$

where V_{ij} is defined by

$$V_{ij} = \Big\{ \boldsymbol{v} \in H^1(\Pi_{ij}) : \ \nabla \cdot \boldsymbol{v} = 0 \text{ in } \Pi_{ij}, \ \boldsymbol{v} = \boldsymbol{U}^i + R\omega^j (n^i_1 \boldsymbol{e}_2 - n^i_2 \boldsymbol{e}_1) \text{ on } \partial B^i, \\ \boldsymbol{v} = \boldsymbol{U}^j + R\omega^i (n^j_1 \boldsymbol{e}_2 - n^j_2 \boldsymbol{e}_1) \text{ on } \partial B^j \ (j \in \mathbb{I}) \text{ or } \boldsymbol{v} = \boldsymbol{f} \text{ on } \partial B^j \ (j \in \mathbb{B}) \\ \frac{1}{R} \int_{\ell_{ij}} \boldsymbol{v} \cdot \boldsymbol{n} ds = \beta^*_{ij} \Big\}, \tag{2.29}$$

with $\boldsymbol{U}^i$, ω^i and β^*_{ij} to be components of some no longer arbitrary but fixed triple $(\mathbb{U}, \boldsymbol{\omega}, \boldsymbol{\beta}^*) \in \boldsymbol{\mathcal{R}}^*$. Functions from V_{ij} are defined in a single neck $\Pi_{ij} \in \boldsymbol{\Pi}$. By direct computations vector fields

$$\begin{aligned} \boldsymbol{u}_t &= \frac{1}{2}(\boldsymbol{U}^i + \boldsymbol{U}^j), \\ \boldsymbol{u}_{sh} &= [(\boldsymbol{U}^i - \boldsymbol{U}^j)\cdot \boldsymbol{p}^{ij}]\boldsymbol{u}_1 + R(\omega^i + \omega^j)\boldsymbol{u}_3, \\ \boldsymbol{u}_{sq} &= [(\boldsymbol{U}^i - \boldsymbol{U}^j)\cdot \boldsymbol{q}^{ij}]\boldsymbol{u}_2, \\ \boldsymbol{u}_{per} &= R(\omega^i - \omega^j)\boldsymbol{u}_4 + \boldsymbol{u}_p, \end{aligned} \tag{2.30}$$

are orthogonal with respect to the scalar product induced by the dissipation functional $W_{\Pi_{ij}}$:

$$\begin{aligned} W_{\Pi_{ij}}(\boldsymbol{u}) = W_{\Pi_{ij}}(\boldsymbol{u}_{sh}) + W_{\Pi_{ij}}(\boldsymbol{u}_{sq}) + W_{\Pi_{ij}}(\boldsymbol{u}_{per}), \quad W_{\Pi_{ij}}(\boldsymbol{u}_t) = 0, \\ \boldsymbol{u} = \boldsymbol{u}_t + \boldsymbol{u}_{sh} + \boldsymbol{u}_{sq} + \boldsymbol{u}_{per}. \end{aligned} \tag{2.31}$$

Physically, the decomposition (2.31) corresponds to three well-known types of microflows. Namely, (i) the shear type arises when a pair of inclusions either rotates in the same direction or disks move into opposite directions (Fig. 2.8a, 2.7a), (ii) the squeeze type, when two inclusions in a pair move towards or away from each other in thin gaps (Fig. 2.7b), (iii) and permeation of the fluid through the thin gaps between neighbors due to Poiseuille flow between motionless inclusions or rotation of neighbors in the opposite directions (Fig. 2.10, 2.8b).

We are now ready to introduce a quadratic form which determines the discrete dissipation rate. To this end from now on instead of β^*_{ij} as a discrete variable we will use:

$$\beta_{ij} = \beta^*_{ij} - \frac{\delta_{ij}}{2R}\left[(\boldsymbol{U}^i + \boldsymbol{U}^j)\cdot \boldsymbol{p}^{ij}\right] - (\omega^i - \omega^j)\frac{\delta_{ij}}{2R}\left[1 + \frac{\delta_{ij}}{4R}\right]. \tag{2.32}$$

The reason for this replacement is that β_{ij} is invariant with respect to Galilean transformation whereas β^*_{ij} is not (see remark in the end of Subsection 6.1 of [10]). For example, if a constant vector $\boldsymbol{U}^0$ is added to both $\boldsymbol{U}^i$ and $\boldsymbol{U}^j$ then the total flux β^*_{ij} changes while β_{ij} stays the same. Also, β^*_{ij} is the total flux through ℓ_{ij} of the entire flow (including the parallel translation, shear, squeeze and permeation) whereas β_{ij} is the flux due to the Poiseuille microflow solely. Finally, the use of β_{ij} simplifies the discrete dissipation form (equation (2.36)).

The use of β_{ij} instead of β^*_{ij} leads to the replacement of the class $\boldsymbol{\mathcal{R}}^*$ (2.27) by $\boldsymbol{\mathcal{R}}$ defined as follows:

$$\begin{aligned} \boldsymbol{\mathcal{R}} = \big\{(\mathbb{U}, \boldsymbol{\omega}, \boldsymbol{\beta})\colon \boldsymbol{U}^i, \omega^i \text{ satisfying boundary condition on } \partial\Omega \text{ (2.14) for } i \in \mathbb{B}, \\ (\mathbb{U}, \boldsymbol{\beta}) \text{ satisfying weak incompresibility condition (2.17), (2.32)}\big\}. \end{aligned} \tag{2.33}$$

Introduce the *effective discrete dissipation rate*:

$$\mathcal{I} := Q(\widehat{\mathbb{U}}, \widehat{\boldsymbol{\omega}}, \widehat{\boldsymbol{\beta}}) = \min_{(\mathbb{U}, \boldsymbol{\omega}, \boldsymbol{\beta}) \in \boldsymbol{\mathcal{R}}} Q(\mathbb{U}, \boldsymbol{\omega}, \boldsymbol{\beta}), \tag{2.34}$$

where

$$Q(\mathbb{U},\boldsymbol{\omega},\boldsymbol{\beta}) = \sum_{i\in\mathbb{I}}\sum_{j\in\mathcal{N}_i} Q_{ij}, \tag{2.35}$$

$$\begin{aligned}
Q_{ij}(\boldsymbol{U}^i,\boldsymbol{U}^j,\omega^i,\omega^j,\beta_{ij}) &= \left[(\boldsymbol{U}^i-\boldsymbol{U}^j)\cdot\boldsymbol{p}^{ij}+R\omega^i+R\omega^j\right]^2\boldsymbol{\mathcal{C}}_1^{ij}\delta^{-1/2}\\
&+\left[(\boldsymbol{U}^i-\boldsymbol{U}^j)\cdot\boldsymbol{q}^{ij}\right]^2\left(\boldsymbol{\mathcal{C}}_2^{ij}\delta^{-3/2}+\boldsymbol{\mathcal{C}}_3^{ij}\delta^{-1/2}\right)\\
&+\beta_{ij}^2\left(\boldsymbol{\mathcal{C}}_4^{ij}\delta^{-5/2}+\boldsymbol{\mathcal{C}}_5^{ij}\delta^{-3/2}+\boldsymbol{\mathcal{C}}_6^{ij}\delta^{-1/2}\right)\\
&+R(\omega^i-\omega^j)\beta_{ij}\left(\boldsymbol{\mathcal{C}}_7^{ij}\delta^{-3/2}+\boldsymbol{\mathcal{C}}_8^{ij}\delta^{-1/2}\right)\\
&+R^2(\omega^i-\omega^j)^2\boldsymbol{\mathcal{C}}_9^{ij}\delta^{-1/2},\quad \text{for } j\in\mathcal{N}_i\cap\mathbb{I},
\end{aligned} \tag{2.36}$$

$$\begin{aligned}
Q_{ij}(\boldsymbol{U}^i,\omega^i,\beta_{ij},\boldsymbol{f}) &= \beta_{ij}^2\left[\boldsymbol{\mathcal{B}}_1^{ij}\delta^{-5/2}+\boldsymbol{\mathcal{B}}_2^{ij}\delta^{-3/2}+\boldsymbol{\mathcal{B}}_3^{ij}\delta^{-1/2}\right]\\
&+\left[(\boldsymbol{U}^i-\boldsymbol{U}^j)\cdot\boldsymbol{p}^{ij}+R\omega^i\right]^2\boldsymbol{\mathcal{B}}_4^{ij}\delta^{-1/2}\\
&+R^2(\omega^i-\omega^j)^2\boldsymbol{\mathcal{B}}_5^{ij}\delta^{-1/2}\\
&+\left[(\boldsymbol{U}^i-\boldsymbol{U}^j)\cdot\boldsymbol{q}^{ij}\right]^2\left(\boldsymbol{\mathcal{B}}_6^{ij}\delta^{-3/2}+\boldsymbol{\mathcal{B}}_7^{ij}\delta^{-1/2}\right)\\
&+\beta_{ij}\left[(\boldsymbol{U}^i-\boldsymbol{U}^j)\cdot\boldsymbol{p}^{ij}+R\omega^i\right](\boldsymbol{\mathcal{B}}_8^{ij}\delta^{-3/2}+\boldsymbol{\mathcal{B}}_9^{ij}\delta^{-1/2})\\
&+\beta_{ij}R(\omega^i-\omega^j)(\boldsymbol{\mathcal{B}}_{10}^{ij}\delta^{-3/2}+\boldsymbol{\mathcal{B}}_{11}^{ij}\delta^{-1/2})\\
&+\beta_{ij}R\omega^i\boldsymbol{\mathcal{B}}_{12}^{ij}\delta^{-1/2}\\
&+\left[(\boldsymbol{U}^i-\boldsymbol{U}^j)\cdot\boldsymbol{p}^{ij}+R\omega^i\right]R(\omega^i-\omega^j)\boldsymbol{\mathcal{B}}_{13}^{ij}\delta^{-1/2}\\
&+\left[(\boldsymbol{U}^i-\boldsymbol{U}^j)\cdot\boldsymbol{q}^{ij}\right]Ra\boldsymbol{\mathcal{B}}_{14}^{ij}\delta^{-1/2},\quad \text{for } j\in\mathcal{N}_i\cap\mathbb{B},
\end{aligned} \tag{2.37}$$

called the *discrete dissipation rates*, with coefficients $\boldsymbol{\mathcal{C}}_k^{ij}$, $k=1,\dots,9$, $\boldsymbol{\mathcal{B}}_m^{ij}$, $m=1,\dots,14$, which depend on μ, the ratio $\dfrac{R}{d_{ij}}$ and explicitly given by (A.1) in Appendix.

The solution of the discrete problem (2.34) is a set of discrete variables $(\widehat{\mathbb{U}},\widehat{\boldsymbol{\omega}},\widehat{\boldsymbol{\beta}})\in\mathcal{R}$, where $\widehat{\mathbb{U}}$ represents the set of translational velocities of inclusions, $\widehat{\boldsymbol{\omega}}$ the set of angular velocities and $\widehat{\boldsymbol{\beta}}$ characterizes the Poiseuille microflow in necks between neighboring inclusions.

Remark 2.2. $Q(\mathbb{U},\boldsymbol{\omega},\boldsymbol{\beta})$, defined by (2.35), is a positive definite quadratic form (see Appendix C.1 of [10]).

Remark 2.3. The agreement of the coefficients in (2.36) (explicitly given in (A.1)) with the previous results of [7] is as follows. Only coefficients $\boldsymbol{\mathcal{C}}_1^{ij}$, $\boldsymbol{\mathcal{C}}_2^{ij}$ coincide with the corresponding coefficients C_{sh}^{ij}, C_{sp}^{ij} in [7]. This is because the coefficients in [7] are obtained by using the approximation of circular surfaces of inclusions by parabolas whereas in this paper we use the true circular surfaces. The main objective of [7] was capturing the strong blow up

term of order $\delta^{-3/2}$ only, which requires coefficients C_{sp}^{ij} ($\boldsymbol{\mathcal{C}}_2^{ij}$). The parabolic approximation does not bring any discrepancy in C_{sp}^{ij} whereas it may bring a discrepancy in some other coefficients. Also since in [7] only the leading term was considered under special boundary conditions there was no need to consider the Poiseuille microflow.

Both Theorems 2.1 and 2.2 are based on the following technical proposition.

Proposition 2.1. *Suppose Ω_F satisfies the close packing condition. Let the triple $(\widehat{\mathbb{U}}, \widehat{\boldsymbol{\omega}}, \widehat{\boldsymbol{\beta}}) \in \boldsymbol{\mathcal{R}}$ solve the discrete problem* (2.34)-(2.37)*. Then the following estimate holds:*

$$|\widehat{W} - \mathcal{I}| \leq \mu \left(\sum_{i \in \mathbb{I}} \sum_{j \in \mathcal{N}_i} C_1 \widehat{\beta}_{ij}^2 + C_2 |\widehat{\boldsymbol{U}}^i - \widehat{\boldsymbol{U}}^j|^2 + C_3 \sum_{i \in \mathbb{I} \cup \mathbb{B}} R^2 (\widehat{\omega}^i)^2 \right). \quad (2.38)$$

where C_k, $k = 1, 2, 3$, are dimensionless constants.

The quadratic form Q defined by (2.35)-(2.37) can be written in the following form:

$$Q = Q_{sh}^{in} + Q_{sq}^{in} + Q_{per}^{in} + Q_{per}^{b} + Q_{sq}^{b}, \quad (2.39)$$

where

$$Q_{sh}^{in} = \sum_{i \in \mathbb{I}} \sum_{j \in \mathcal{N}_i \cap \mathbb{I}} \left[(\boldsymbol{U}^i - \boldsymbol{U}^j) \cdot \boldsymbol{p}^{ij} + R\omega^i + R\omega^j \right]^2 \boldsymbol{\mathcal{C}}_1^{ij} \delta^{-1/2},$$

$$Q_{sq}^{in} = \sum_{i \in \mathbb{I}} \sum_{j \in \mathcal{N}_i \cap \mathbb{I}} \left[(\boldsymbol{U}^i - \boldsymbol{U}^j) \cdot \boldsymbol{q}^{ij} \right]^2 \left(\boldsymbol{\mathcal{C}}_2^{ij} \delta^{-3/2} + \boldsymbol{\mathcal{C}}_3^{ij} \delta^{-1/2} \right),$$

$$\begin{aligned} Q_{per}^{in} = \sum_{i \in \mathbb{I}} \sum_{j \in \mathcal{N}_i \cap \mathbb{I}} \Big\{ & \beta_{ij}^2 \left(\boldsymbol{\mathcal{C}}_4^{ij} \delta^{-5/2} + \boldsymbol{\mathcal{C}}_5^{ij} \delta^{-3/2} + \boldsymbol{\mathcal{C}}_6^{ij} \delta^{-1/2} \right) \\ & + R(\omega^i - \omega^j) \beta_{ij} \left(\boldsymbol{\mathcal{C}}_7^{ij} \delta^{-3/2} + \boldsymbol{\mathcal{C}}_8^{ij} \delta^{-1/2} \right) \\ & + R^2 (\omega^i - \omega^j)^2 \boldsymbol{\mathcal{C}}_9^{ij} \delta^{-1/2} \Big\} \end{aligned}$$

$$\begin{aligned} Q_{per}^{b} = \sum_{i \in \mathbb{I}} \sum_{j \in \mathcal{N}_i \cap \mathbb{B}} \Big\{ & \beta_{ij}^2 \left[\boldsymbol{\mathcal{B}}_1^{ij} \delta^{-5/2} + \boldsymbol{\mathcal{B}}_2^{ij} \delta^{-3/2} + \boldsymbol{\mathcal{B}}_3^{ij} \delta^{-1/2} \right] \\ & + \boldsymbol{\mathcal{B}}_8^{ij} \beta_{ij} \left[(\boldsymbol{U}^i - \boldsymbol{U}^j) \cdot \boldsymbol{p}^{ij} + R\omega^i \right] \delta^{-3/2} + \boldsymbol{\mathcal{B}}_{10}^{ij} \beta_{ij} R(\omega^i - \omega^j) \delta^{-3/2} \\ & + \boldsymbol{\mathcal{B}}_9^{ij} \beta_{ij} \left[(\boldsymbol{U}^i - \boldsymbol{U}^j) \cdot \boldsymbol{p}^{ij} + R\omega^i \right] \delta^{-1/2} + \boldsymbol{\mathcal{B}}_{11}^{ij} \beta_{ij} R(\omega^i - \omega^j) \delta^{-1/2} \\ & + \boldsymbol{\mathcal{B}}_{12}^{ij} \beta_{ij} R\omega^i \delta^{-1/2} + \boldsymbol{\mathcal{B}}_4^{ij} \left[(\boldsymbol{U}^i - \boldsymbol{U}^j) \cdot \boldsymbol{p}^{ij} + R\omega^i \right]^2 \delta^{-1/2} \\ & + \boldsymbol{\mathcal{B}}_{13}^{ij} \left[(\boldsymbol{U}^i - \boldsymbol{U}^j) \cdot \boldsymbol{p}^{ij} + R\omega^i \right] R(\omega^i - \omega^j) \delta^{-1/2} \\ & + \boldsymbol{\mathcal{B}}_5^{ij} R^2 (\omega^i - \omega^j)^2 \delta^{-1/2} \Big\}, \end{aligned}$$

$$Q^b_{sq} = \sum_{i\in\mathbb{I}} \sum_{j\in\mathcal{N}_i\cap\mathbb{B}} \Big\{ \left[(\boldsymbol{U}^i - \boldsymbol{U}^j)\cdot \boldsymbol{q}^{ij}\right]^2 \left(\boldsymbol{\mathcal{B}}^{ij}_6 \delta^{-3/2} + \boldsymbol{\mathcal{B}}^{ij}_7 \delta^{-1/2}\right) + \boldsymbol{\mathcal{B}}^{ij}_{14} \left[(\boldsymbol{U}^i - \boldsymbol{U}^j)\cdot \boldsymbol{q}^{ij}\right] Ra\delta^{-1/2} \Big\}. \tag{2.40}$$

Remark 2.4. Both Q^{in}_{per} and Q^b_{per} are quadratic forms (see Appendix I of [10]).

Remark 2.5. The discrete dissipation rate $\mathcal{I}$ makes physics transparent. We can see how microflows enter this dissipation rate. Indeed, the *discrete dissipation form* Q is presented as a sum of three motions corresponding to the decomposition (2.31). The decomposition (2.39) reflects the physics of the problem. Namely, for the interior necks the first term Q^{in}_{sh} corresponds to the dissipation rate $W_{\Pi_{ij}}(\boldsymbol{u}_{sh})$ in (2.31) and describes the shear flow between inclusions. This type of flow is produced by two motions: rotation in the same direction (Fig. 2.8*a*) and relative shear (Fig. 2.7*a*). The second term Q^{in}_{sq} corresponds to the dissipation rate $W_{\Pi_{ij}}(\boldsymbol{u}_{sq})$ in (2.31) and describes the local flow due to the squeeze motion (Fig. 2.7*b*). The third term Q^{in}_{per} corresponds to the dissipation rate $W_{\Pi_{ij}}(\boldsymbol{u}_{per})$ in (2.31) and describes the "permeation" type flow due to the Poiseuille microflow between motionless inclusions (Fig. 2.10) and the rotation into the opposite directions (Fig. 2.8*b*). Finally, the last term Q_b describes the local flow in the thin gap between a disk and the external boundary. Here the decomposition into the parts corresponding to permeation Q^b_{per} and squeeze Q^b_{sq} in boundary necks is similar to one in interior necks.

Remark 2.6. The asymptotics (2.38) is given in terms of the *discrete dissipation rates* Q_{ij}. These dissipation rates are quadratic forms of the key physical parameters $\mathbb{U}, \boldsymbol{\omega}, \boldsymbol{\beta}$. In particular, the effective discrete dissipation rate reveals the functional dependence of the effective properties of suspensions on the microflows (the shear, squeeze and permeation between neighbors).

3 Anomalous Rate of Blow up of the Dissipation Rate, Qualitative Conclusions, Discussions and Open Problems

In this section we show that in 3D the Poiseuille microflow does not occur (the fluid simply flows around the neck). In contrast, in 2D incompressible fluid may need to permeate through necks. Necks separate fluid domain into *disconnected* regions, triangles, which may have different pressures p_1, p_2 (Fig. 3.1). In this sense, the 2D problem becomes more complicated than an analogous 3D problem. Moreover, this type of flow in experimental 2D settings may lead to an observable physical effect.

In the previous study [7] of 2D flow only the strong blow up term of order $O(\delta^{-3/2})$ of the asymptotics of the effective viscosity was captured. The subsequent study of [13] reveals the significance of the weak blow up of order $O(\delta^{-1/2})$ in 2D. It was shown that it becomes the leading term in the asymptotics of the shear effective viscosity. The objectives of [13] was to study the

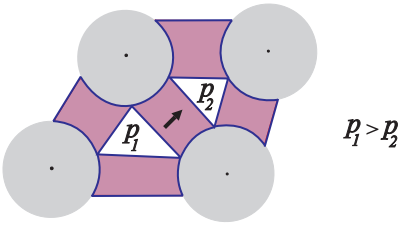

Fig. 3.1. Local flux due to pressure drop

degeneracy of the strong blow up term and evaluate the order of the magnitude of the next term which was shown to exhibit the weak blow up. The qualitative conclusion of the analysis of [13] was that the shear viscosity exhibits the weak blow up in both 2D and 3D. While this study highlighted the significance of the weak blow up term, it was not calculated there. As shown in Theorem 2.1 above the fictitious fluid approach suggested in this paper allows to calculate ***any*** singular term, and, in particular, the weak blow up. While a generalization of techniques of [7] for 3D suspensions leads to increasing technical difficulties, the fictitious fluid approach provides an appropriate tool to attack this problem. We anticipate that this approach would also be useful in a variety of similar physical problems (e.g. rigid inclusions in an elastic medium in both 2D and 3D). Moreover, the analysis by this approach reveals the significance of the Poiseuille microflows. In this section we present an example which illustrates the following. For the suspensions of free inclusions the Poiseuille microflows contribute to the weak blow up. However, if an external field, which "clamps" inclusions, is imposed on inclusions then the Poiseuille microflow may result in a new type singular behavior of viscous dissipation rate (superstrong blow up). We also present an example of one disk in the fluid that can be clamped by the fluid flow with no external field. However, it is not clear whether this example can be generalized to an ensemble of inclusions. Our example may suggest that on a suspension of free inclusions the superstrong blow up may occur only due to boundary layer effects and therefore for the large number of inclusions becomes negligible.

3.1 Suspensions in a Pinning Field

Example 3.1. The techniques described above can be applied to the problems of suspensions of non-neutrally buoyant rigid inclusions defined by

$$
\begin{aligned}
&(a)\ \mu\triangle \boldsymbol{u} = \nabla p, && \boldsymbol{x}\in\Omega_F\\
&(b)\ \nabla\cdot\boldsymbol{u} = 0, && \boldsymbol{x}\in\Omega_F\\
&(c)\ \boldsymbol{u} = \boldsymbol{U}^i + R\omega^i(n_1^i\boldsymbol{e}_2 - n_2^i\boldsymbol{e}_1), && \boldsymbol{x}\in\partial B^i,\quad i=1\dots N\\
&(d)\ \int_{\partial B^i}\boldsymbol{\sigma}(\boldsymbol{u})\boldsymbol{n}^i ds = m\boldsymbol{g}, && i=1\dots N\\
&(e)\ \int_{\partial B^i}\boldsymbol{n}^i\times\boldsymbol{\sigma}(\boldsymbol{u})\boldsymbol{n}^i ds = 0, && i=1\dots N\\
&(f)\ \boldsymbol{u} = \boldsymbol{f}, && \boldsymbol{x}\in\partial\Omega
\end{aligned}
\tag{3.1}
$$

where the domain Ω_F is depicted in Fig. 3.2, where m, $\boldsymbol{g}$ are given constant, constant vector field, respectively. This problem corresponds to minimization of $W_{\Omega_F}(\boldsymbol{u}) + \sum_{i=1}^{N} m\boldsymbol{g}\cdot\boldsymbol{U}^i$. The additional term does not change the analysis.

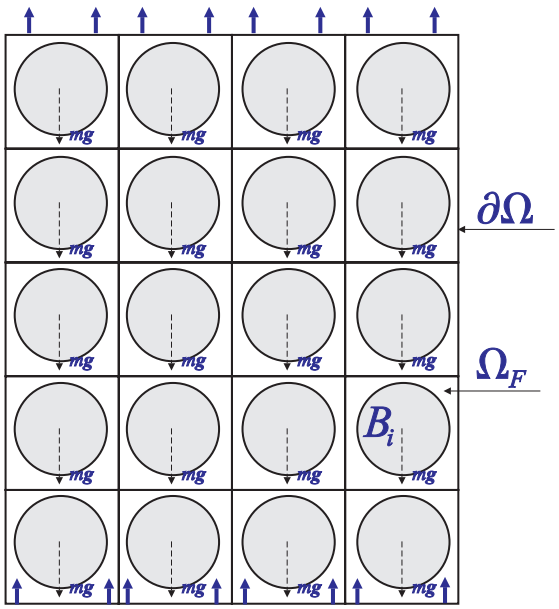

Fig. 3.2. Example of a domain occupied by a suspension in a presence of a pinning field (gravity)

Here we suppose that the density of the solid inclusions is ρ_s and the fluid density is ρ_f. Then the force on the inclusion in the left hand side of (3.1d) counteracts the external gravitational field $-m\boldsymbol{g}$, where $\boldsymbol{g} = (0, g)$ is acceleration due to the gravity and $m = \pi R^2(\rho_s - \rho_f)$ is the excess mass. We choose the external boundary condition $\boldsymbol{f}$ and the force exerted by the heavy disks on the fluid so that the inclusions do not move and fluid is forced

to permeate through the thin gaps between motionless inclusions. The force exerted by the disks is equal to their weight $\pi R^2(\rho_s - \rho_f)g$, where we choose inclusions to be superheavy:

$$\rho_s = C\delta^{-5/2}, \text{ for some } C = C(\mu, R) > 0, \tag{3.2}$$

and the applied boundary data $\boldsymbol{f}$ is chosen so that

$$\boldsymbol{f} = \begin{pmatrix} 0 \\ f_2(x,y) \end{pmatrix} \in H^{1/2}(\partial\Omega), \tag{3.3}$$

where f_2 is some periodic function of $(x, y) \in \partial\Omega$. Such a boundary data $\boldsymbol{f}$ and the asymptotics of ρ_s are selected so that inclusions do not move (the gravity balances the viscous force). This balance can be found by solving an auxiliary problem similar to the one considered in [35] (for details see Appendix A.4 of [10]).

Then the following proposition holds.

Proposition 3.2 (*Superstrong Blow Up due to a Pinning Field*). *Let $\widehat{W}$ be the effective viscous dissipation rate of the problem* (3.1)*. There exist ρ_s and $\boldsymbol{f}$ of the form* (3.2) *and* (3.3)*, respectively, such that the following asymptotic representation holds:*

$$\widehat{W} = N\left(\mathcal{C}_1\delta^{-5/2} + \mathcal{C}_2\delta^{-3/2} + \mathcal{C}_3\delta^{-1/2}\right) + O(1), \quad \textit{as} \quad \delta \to 0,$$

$$\textit{where } \mathcal{C}_1 = \frac{9}{4}\pi\mu R^{5/2}, \mathcal{C}_2 = \frac{99}{160}\pi\mu R^{3/2}, \mathcal{C}_2 = \frac{29241}{17920}\pi\mu R^{1/2},$$

and N is the total number of inclusions.

The proof of this proposition can be found in Appendix A.4 of [10].

3.2 No Singularity of the Dissipation Rate due to the Poiseuille Microflow in 3D

Example 3.2. In order to explain why the the Poiseuille microflow does not contribute to the singular behavior of the dissipation rate in 3D let us consider what happens with the fluid between two neighboring inclusions. Let $K = [-L, L]^3$ be a cube. The parts of two neighboring inclusions are modeled by the hemispheres attached to the top and bottom faces of the cube as shown in Fig. 3.3. Consider a 3D analog of the problem (2.1) with boundary condition $\boldsymbol{f}$ to be a given constant vector $\boldsymbol{V}$ on two opposite sides of the lateral boundary and zero vector on the rest of the boundary (Fig. 3.3). Since the effective viscous dissipation rate $\widehat{W}$ is bounded from above by the dissipation rate $W(\boldsymbol{w})$ for any test function $\boldsymbol{w}$ it suffices to find $\boldsymbol{w}$ such that $W(\boldsymbol{w}) = O(1)$.

Consider a "hourglass domain" Ψ inside of the box containing two hemispheres as in Fig. 3.3. We choose the trial function $\boldsymbol{w}$ to be:

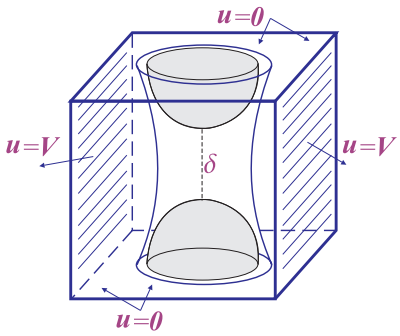

Fig. 3.3. Poiseuille microflow in 3D

$$\boldsymbol{w} = \begin{cases} \mathbf{0}, & \text{when } \boldsymbol{x} \in \Psi \\ \boldsymbol{W}, & \text{when } \boldsymbol{x} \in K \setminus \Psi \end{cases} \tag{3.4}$$

where $\boldsymbol{W}$ solves the Stokes problem with Dirichlet boundary conditions: $\boldsymbol{W} = \mathbf{0}$ on the boundary of Ψ and $\boldsymbol{W} = \boldsymbol{f}$ on ∂K (such a solution exists and is unique).

Evaluating the dissipation rate on such a trial function we obtain:

$$W(\boldsymbol{w}) \le \|\boldsymbol{w}\|^2_{H^1(K)} \le C\|\boldsymbol{V}\|^2_{H^{1/2}(\partial K)} = O(1).$$

3.3 Boundary Layer Effects Leading to Superstrong Blow Up

Example 3.3. Consider the domain $\Omega = (-1,1)^2$ which contains only one inclusion B. Decompose the domain outside B into necks $\bigcup_{i=1}^{4} \Pi_i$ and squares $\bigcup_{i=1}^{4} \square_i$ as in Fig. 3.4(a). Choose

$$\boldsymbol{f} = \begin{cases} \begin{pmatrix} -1 \\ 1 \end{pmatrix} \zeta_1, & \partial\square_1 \cap \partial\Omega =: \Gamma_1 \\ \begin{pmatrix} -1 \\ -1 \end{pmatrix} \zeta_2, & \partial\square_2 \cap \partial\Omega =: \Gamma_2 \\ \begin{pmatrix} 1 \\ -1 \end{pmatrix} \zeta_3, & \partial\square_3 \cap \partial\Omega =: \Gamma_3 \\ \begin{pmatrix} 1 \\ 1 \end{pmatrix} \zeta_4, & \partial\square_4 \cap \partial\Omega =: \Gamma_4 \\ \mathbf{0}, & \text{elsewhere} \end{cases}$$

where ζ_i, $i = 1, \dots, 4$ are smooth function having a compact support outside of Γ_i such that $\zeta_i = 1$ in Γ_i. Moreover, they satisfy the following symmetry condition:

$$\zeta_1(x,y) = \zeta_2(-x,y) = \zeta_3(-x,-y) = \zeta_4(x,-y) \quad \text{and} \quad \zeta_1(x,y) = \zeta_1(y,x).$$

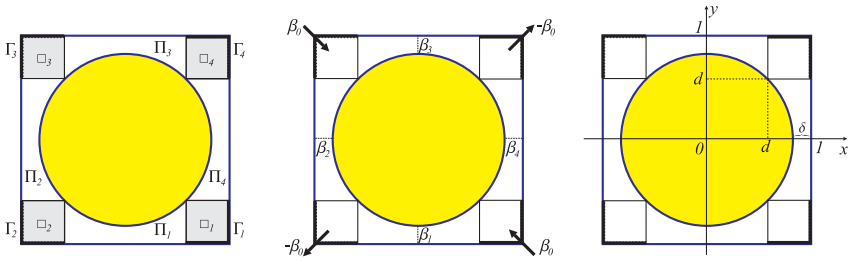

(a) (b) (c)

Fig. 3.4. One inclusion example: Boundary layer lead to superstrong blow up of viscous dissipation rate

The fluxes through the parts of the boundary Γ_1 and Γ_3 which are equal and we denote them by

$$\beta_0 = \frac{2}{R}(-1+d), \quad d = \delta + R(1 - \frac{1}{\sqrt{2}}).$$

Then the fluxes through Γ_2 and Γ_4 are $-\beta_0$.

Due to symmetry of the problem the inclusion does not rotate, that is, $\omega = 0$ and $\beta_1 = \beta_3 = -\beta_2 = -\beta_4$ (see Fig. 3.4(b)). Then

$$\begin{aligned}
\mathcal{I} = \min_{\boldsymbol{U},\beta_i} \sum_{i=1}^{4} & A\delta^{-3/2}[\boldsymbol{U}\cdot\boldsymbol{q}^i]^2 + B\delta^{-1/2}[\boldsymbol{U}\cdot\boldsymbol{p}^i]^2 + CR^2\delta^{-5/2}\beta_i^2 \\
& -p_1(\beta_0 + \beta_1 - \beta_4 + U_1 - U_2) - p_2(-\beta_0 + \beta_2 - \beta_1 - U_1 - U_2) \\
& -p_3(\beta_0 + \beta_3 - \beta_2 - U_1 + U_2) - p_4(-\beta_0 + \beta_4 - \beta_3 + U_1 + U_2) \\
= \min_{\boldsymbol{U},\beta_i} & \{2A\delta^{-3/2}[U_1^2 + U_2^2] + 2B\delta^{-1/2}[U_1^2 + U_2^2] + 4CR^2\delta^{-5/2}\beta_1^2 \\
& -p_1(2\beta_0 + 4\beta_1) - p_2(-2\beta_0 - 4\beta_1)\},
\end{aligned}$$

where p_i, $i = 1, \dots, 4$ are the Lagrange multipliers corresponding to the weak incompressibility condition (2.17) and $p_1 = p_3$, $p_2 = p_4$.

Solving the Euler-Lagrange equations for this minimization problem we obtain

$$U_1 = U_2 = 0, \quad \beta_1 = -\frac{\beta_0}{2} = \frac{1}{R}(1-d),$$

which provides the following asymptotics:

$$\mathcal{I} = C(1-d)^2\delta^{-5/2}.$$

Thus, we see that the superstrong blow up can occur due to the boundary layer where Poiseuille flow is significant.

3.4 Free Suspensions (no external field)

In the above example 3.1 we demonstrated that the Poiseuille microflow dominates the asymptotics of the effective viscous dissipation rate and may cause the superstrong blow up of order $O(\delta^{-5/2})$. The key ingredient of this example is the presence of a strong external pinning field which "clamps" inclusions or alternatively the presence of the boundary layer as in Example 3.3. In typical suspensions, with no external field, the inclusions are free to move. Then we expect that β is asymptotically small, as $\delta \to 0$, so that the Poiseuille microflow does not contribute to the superstrong blow up by Theorem 2.1. This observation is also supported by the analysis of the periodicity cell problem with five inclusions in [8]. Below we present an example of a suspension with a hexagonal periodic array of inclusions and prove that for the extensional external boundary conditions the viscous dissipation rate exhibits the strong blow up $O(\delta^{-3/2})$ since all $\beta_{ij} = 0$. Such a hexagonal array in 2D is a representative of a densely packed array of disks.

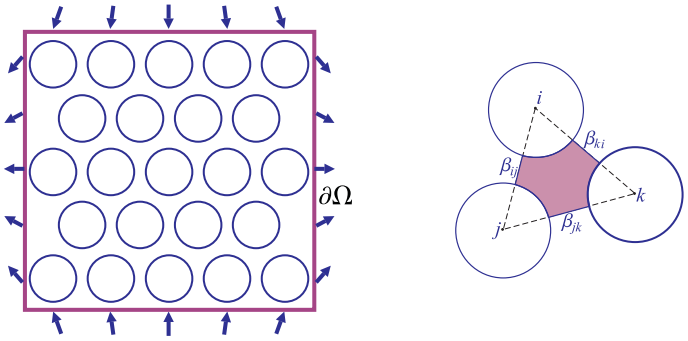

Fig. 3.5. Periodic domain occupied by a suspension under the extensional boundary conditions that exhibits the strong blow up

Example 3.4. Consider a square domain $\Omega = (-M, M)^2$, $M > 0$ with hexagonal array of disks B^i centered at $(x_i, y_i) \in \Omega$ (Fig. 3.5). The boundary value problem (2.1) is supplemented with boundary conditions

$$\boldsymbol{f} = \begin{pmatrix} x \\ -y \end{pmatrix} \quad \text{on} \quad \partial\Omega. \tag{3.5}$$

We first prove that the effective dissipation rate $\widehat{W}_{hex} = O(\delta^{-3/2})$ by constructing a trial vector field $\boldsymbol{v}$ such that $W_{\Omega_F}(\boldsymbol{v}) = O(\delta^{-3/2})$. We thus obtain an upper bound for $\widehat{W}_{hex}$.

The construction is as follows. For each inclusion B^i, centered at $\boldsymbol{x}_i = (x_i, y_i)$ we prescribe the translational velocity to be exactly

$$\boldsymbol{U}^i = \begin{pmatrix} x_i \\ -y_i \end{pmatrix}, \tag{3.6}$$

and the rotational velocity $\omega^i = 0$. For such velocities the zero flux constraint (2.17) for every fluid region $\mathcal{A}_{ijk}$ (see the right part of Fig. 3.5) takes the form

$$\beta_{ij} + \beta_{jk} + \beta_{ki} = 0, \tag{3.7}$$

because elementary computations show that for every i, j, k

$$(\boldsymbol{U}^i + \boldsymbol{U}^j)\boldsymbol{p}^{ij} + (\boldsymbol{U}^j + \boldsymbol{U}^k)\boldsymbol{p}^{jk} + (\boldsymbol{U}^k + \boldsymbol{U}^i)\boldsymbol{p}^{ki} = 0.$$

Hence, we can choose all β_{ij} to be identically zero. Then Theorem 2.1 implies that there exists a trial vector field $\boldsymbol{v}$ such that

$$W_{\Omega_F}(\boldsymbol{v}) = O(\delta^{-3/2}),$$

and, therefore, $\widehat{W}_{hex} = O(\delta^{-3/2})$.

To show that for this array of inclusions $\widehat{W}_{hex} > C\delta^{-3/2}$ we consider a chain of disks that connects upper and lower boundaries of the domain Ω: $\partial\Omega^+ = \{(x, y) : y = M\}$ and $\partial\Omega^-\{(x, y) : y = -M\}$, respectively (see Fig. 3.6). We choose this chain so that the y-axis of the coordinate system passes

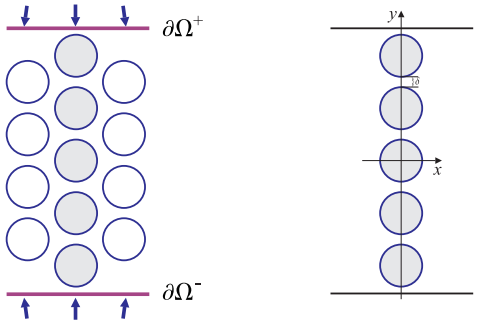

Fig. 3.6. Chain of disks connecting the upper and lower boundaries of Ω

through the centers of disks in this chain. Then

$$\widehat{W} = \min_{\boldsymbol{\mathcal{R}}} Q(\mathbb{U}, \boldsymbol{\omega}, \boldsymbol{\beta}) \geq (\mathcal{C}_2\delta^{-3/2} + \mathcal{C}_3\delta^{-1/2}) \min_{\mathbb{U}} \sum_{chain} (U_2^i - U_2^j)^2.$$

where the last minimum is taken over the disks in the chain (shadowed disks in Fig. 3.6). Then

$$\min_{\mathbb{U}} \sum_{chain} (U_2^i - U_2^j)^2 = A > 0,$$

where A is some constant. Therefore $\widehat{W}_{hex} > C\delta^{-3/2}$. This leads to a conclusion that the effective viscous dissipation rate $\widehat{W}_{per}$ exhibits the strong blow up of order $\delta^{-3/2}$.

It is known that for local movements of pairs of inclusions the squeeze type motion (Fig. 2.7*b*) provides the strongest singularity (of order $\delta^{-3/2}$) whereas all other types of motions: rotations and shear provide a weaker singularity (of order $\delta^{-1/2}$). Thus, it is natural to expect that in a suspension where inclusions are free to move with the extensional boundary conditions the viscous dissipation exhibits the singularity of order $\delta^{-3/2}$. The above example shows that this is indeed the case, that is, the superstrong blow up does not occur and the anomalous rate of $O(\delta^{-5/2})$ can be achieved if an external field is applied.

There is also one more case where the superstrong blow up can be obtained. Namely, Example 3.3 shows that it occurs in the boundary layers. Hence the above $O(\delta^{-3/2})$ conclusion applies to bulk effective properties of free suspensions of large number of inclusions, when the boundary effects are negligible.

4 The Fictitious Fluid Problem

The use of the fictitious fluid approach immediately gives a lower estimate on the viscous dissipation rate $\widehat{W}$ as follows.

Lemma 4.1. *For $\widehat{W}_{\boldsymbol{\Pi}}$ defined by* (2.10) *and $\widehat{W}$ defined by* (2.3) *the following inequality holds:*

$$\widehat{W}_{\boldsymbol{\Pi}} \le \widehat{W}. \tag{4.1}$$

See Section 4 of [10] for the proof of this lemma.

Another significant advantage of the fictitious fluid problem is that the global minimization problem (2.10) can be split into two consecutive problems: one of them is on a single neck Π_{ij}, and the other one is a minimization problem on discrete variables $(\mathbb{U}, \boldsymbol{\omega}, \boldsymbol{\beta}^*) \in \boldsymbol{\mathcal{R}}^*$.

Lemma 4.2. *(Iterative minimization lemma). Suppose $\widehat{W}_{\boldsymbol{\Pi}}$ is defined by* (2.10). *Then*

$$\widehat{W}_{\boldsymbol{\Pi}} = \min_{(\mathbb{U},\boldsymbol{\omega},\boldsymbol{\beta}^*)\in\boldsymbol{\mathcal{R}}^*} \sum_{i\in\mathbb{I}, j\in\mathcal{N}_i} \min_{V_{ij}} W_{\Pi_{ij}}(\cdot), \tag{4.2}$$

where the class $\mathcal{R}^*$ is defined by (2.33). *Moreover, the minimizer of $W_{\Pi_{ij}}$ over V_{ij} satisfies the following Euler-Lagrange equations:*

$$
\begin{aligned}
&(a)\ \mu\triangle \boldsymbol{u} = \nabla p, && \boldsymbol{x}\in \Pi_{ij},\\
&(b)\ \nabla\cdot\boldsymbol{u} = 0, && \boldsymbol{x}\in \Pi_{ij},\\
&(c')\ \boldsymbol{u} = \boldsymbol{U}^i + R\omega^i(n_1^i\boldsymbol{e}_2 - n_2^i\boldsymbol{e}_1), && \boldsymbol{x}\in \partial B^i,\\
&(c'')\ \boldsymbol{u} = \boldsymbol{U}^j + R\omega^j(n_1^j\boldsymbol{e}_2 - n_2^j\boldsymbol{e}_1), && \boldsymbol{x}\in \partial B^j,\\
&(d)\ \frac{1}{R}\int_{\ell_{ij}} \boldsymbol{u}\cdot\boldsymbol{n}ds = \beta_{ij}^*, &&\\
&(e)\ \boldsymbol{\sigma}(\boldsymbol{u})\boldsymbol{n} = -p_{ij}^{\pm}\boldsymbol{n}, && \boldsymbol{x}\in \partial\Pi_{ij}^{\pm},\\
&(f)\ \boldsymbol{u} = \boldsymbol{f}, && \boldsymbol{x}\in \partial\Pi_{ij}\cap\partial\Omega,
\end{aligned}
\tag{4.3}
$$

where $p_{ij}^{\pm}$ are the Lagrange multipliers for the weak incompressibility condition (2.17).

Proof. Minimizing $W_{\boldsymbol{\Pi}}(\boldsymbol{u})$ over $V_{\boldsymbol{\Pi}}$ leads to the Euler-Lagrange equations

$$
\begin{aligned}
&(a)\ \mu\triangle \boldsymbol{u} = \nabla p, && \boldsymbol{x}\in \boldsymbol{\Pi}\\
&(b)\ \nabla\cdot\boldsymbol{u} = 0, && \boldsymbol{x}\in \boldsymbol{\Pi}\\
&(c)\ \boldsymbol{u} = \boldsymbol{U}^i + R\omega^i(n_1^i\boldsymbol{e}_2 - n_2^i\boldsymbol{e}_1), && \boldsymbol{x}\in \partial B^i,\quad i=1\dots N\\
&(d)\ \int_{\partial B^i}\boldsymbol{\sigma}(\boldsymbol{u})\boldsymbol{n}^i ds = \boldsymbol{0} && i=1\dots N\\
&(e)\ \int_{\partial B^i}\boldsymbol{n}^i\times\boldsymbol{\sigma}(\boldsymbol{u})\boldsymbol{n}^i ds = \boldsymbol{0}, && i=1\dots N\\
&(f)\ \int_{\partial\triangle_{ijk}}\boldsymbol{u}\cdot\boldsymbol{n}ds = 0, && i\in\mathbb{I},\ j,k\in\mathcal{N}_i\\
&(g)\ \boldsymbol{\sigma}(\boldsymbol{u})\boldsymbol{n} = p_{ijk}\boldsymbol{n}, && \boldsymbol{x}\in\partial\triangle_{ijk}\\
&(h)\ \boldsymbol{u} = \boldsymbol{f}, && \boldsymbol{x}\in\partial\Omega,
\end{aligned}
\tag{4.4}
$$

where the "pressure constants" p_{ijk} arise from weak incompressibility condition (2.7). Given the boundary data $\boldsymbol{f}$ in (4.4) we uniquely determine (see Appendix C.3 of [10]) unknowns

$$
\boldsymbol{u},\ p,\ \boldsymbol{U}^i,\ \omega^i,\ p_{ijk},\qquad i\in\mathbb{I},\ j,k\in\mathcal{N}_i. \tag{4.5}
$$

Fix a neck Π_{ij} and consider the problem (4.3) on it. For this pair of indices i,j take

$$
\boldsymbol{f},\ \boldsymbol{U}^i,\ \omega^i,\ \boldsymbol{U}^j,\ \omega^j,\ \beta_{ij}^* = \frac{1}{R}\int_{\ell_{ij}}\boldsymbol{u}\cdot\boldsymbol{n}ds \tag{4.6}
$$

found from (4.5). Using (4.6) as a given data, boundary value problem (4.3) can be solved uniquely (see Appendix C.4 of [10]). Due to the unique solvability of both (4.4) and (4.3) the pair $(\boldsymbol{u},p)$ in (4.5) must solve (4.3) and [5]

$$
p_{ij}^{+} = p_{ijk},\quad p_{ij}^{-} = p_{ijm},
$$

[5] For notational convenience we identify $p_{ij}^{+} = p_{jk}^{+} = p_{ki}^{+} = p_{ijk}$, and $p_{ij}^{+} = p_{ji}^{-}$.

where triangles $\triangle_{ijk}$ and $\triangle_{ijm}$ are adjacent to the neck Π_{ij} (see Fig.4.1). Hence (4.4) reduces to (4.3).

At this point the completion of the proof would have been trivial if we did not have β^*_{ij}. Indeed, in the entire domain Ω_F a result analogous to (4.2) is simply

$$\min_{(\mathbb{U},\boldsymbol{\omega},\boldsymbol{u})} W_{\Omega_F}(\boldsymbol{u}) = \min_{(\mathbb{U},\boldsymbol{\omega})} \left(\min_{\boldsymbol{u},\ \text{when } (\mathbb{U},\boldsymbol{\omega}) \text{ fixed}} W_{\Omega_F}(\boldsymbol{u}) \right).$$

Hence it only remains to show that for any given $(\mathbb{U},\boldsymbol{\omega})$ we can find at least one set $\boldsymbol{\beta}^*$ satisfying the weak incompressibility condition (2.17). To this end we fix $(\mathbb{U},\boldsymbol{\omega})$ and let $\boldsymbol{u}$ be the solution of the Stokes equation $\mu\triangle\boldsymbol{u} = \nabla p$ and $\nabla\cdot\boldsymbol{u} = 0$ in the domain Ω_F with the Dirichlet data $\boldsymbol{u}|_{\partial B^i} = \boldsymbol{U}^i + R\omega^i(n^i_1\boldsymbol{e}_2 - n^i_2\boldsymbol{e}_1)$, $\boldsymbol{u}|_{\partial\Omega} = \boldsymbol{f}$. Set $\beta^*_{ij} = \dfrac{1}{R}\displaystyle\int_{\ell_{ij}} \boldsymbol{u}\cdot\boldsymbol{n}ds$. Hence, we obtain $\boldsymbol{\beta}^* = \{\beta^*_{ij}\}$ such that $(\mathbb{U},\boldsymbol{\omega},\boldsymbol{\beta}^*) \in \boldsymbol{\mathcal{R}}^*$. This completes the proof of lemma 4.2.

Remark 4.7. For a given $(\mathbb{U},\boldsymbol{\omega})$ permeation constants $\boldsymbol{\beta}^*$ may not be unique. In fact, the choice of β^*_{ij} has N degrees of freedom where N is the number of inclusions. Indeed, $\boldsymbol{\beta}^*$ is found from solving a linear system $A\boldsymbol{\beta}^* = \boldsymbol{b}$ where the number of unknowns equals the number P of interior necks and the number of equations equals the number of triangles, but there are only $P-N$ linearly independent ones. Hence, the number of free parameters is equal to the number of inclusions.

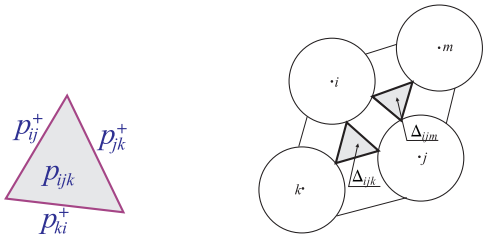

Fig. 4.1. (a) Pressures on the boundary of the triangle $\triangle_{ijk}$; (b) Two triangles adjacent to the neck Π_{ij}

Remark 4.8. The unknowns of the problem (4.4) are the velocity field $\boldsymbol{u}(\boldsymbol{x})$, the pressure $p(\boldsymbol{x})$, the constant translational $\boldsymbol{U}^i$ and angular ω^i velocities of the disk B^i, $i = 1,\dots,N$ and constants p_{ijk}. Formally these constants appear as the Lagrange multipliers for the constraints (2.7). Similar to how the pressure $p(\boldsymbol{x})$ appears as the Lagrange multiplier in the variational formulation corresponding to the Stokes equation, the weak incompressibility condition

for the fictitious fluid, inherited from the original fluid, gives rise to the constant Lagrange multipliers, that one can regard as a constant pressure on the boundary of the fictitious fluid domain. This also motivates the notations p_{ijk}. Thus, the fictitious fluid may be also interpreted as follows: an incompressible fluid occupies necks while triangular pockets are filled with "gas" of the constant pressure p_{ijk}. Naturally, the unknowns of the problem (4.3) are the functions $\boldsymbol{u}(\boldsymbol{x})$, $p(\boldsymbol{x})$ and constants $p_{ij}^{\pm}$, representing the velocity field, the pressure in the neck Π_{ij} and the constant pressures on the lateral boundary $\partial\Pi_{ij}^{\pm}$, respectively.

Remark 4.9. A major difficulty in applying previous "one-step" discretization techniques [7, 11, 12] to vectorial problems is the presence of integral constraints in the dual variational formulation. In the described "two-step" discretization approach, due to the Iterative Minimization Lemma, the inner minimization problem has Dirichlet boundary conditions on inclusions and therefore neither this problem, nor its dual have any integral conditions. On the other hand, due to (4.2) second minimization implies that these integral conditions are automatically satisfied.

Lemma 4.3. *Suppose Ω_F satisfies the close packing condition. Then for $\widehat{W}_{\boldsymbol{\Pi}}$ defined by* (2.10) *and $\widehat{W}$ defined by* (2.3) *the following inequality holds:*

$$\widehat{W} \leq \widehat{W}_{\boldsymbol{\Pi}} + \mu \left(\sum_{i\in\mathbb{I}} \sum_{j\in\mathcal{N}_i} C_1 R^2 \widehat{\beta}_{ij}^2 + C_2 |\widehat{\boldsymbol{U}}^i - \widehat{\boldsymbol{U}}^j|^2 + C_3 \sum_{i\in\mathbb{I}\cup\mathbb{B}} R^2 (\widehat{\omega}^i)^2 \right), \tag{4.7}$$

where $(\widehat{\mathbb{U}}, \widehat{\boldsymbol{\omega}}, \widehat{\boldsymbol{\beta}}^*)$ minimizes (4.2).

The proof of this lemma relies on the technical construction that appears in the proof of Lemma 5.4 of the next section. For simplicity of the presentation here we omit both proofs which can be found in Chapter 6 of [10].

Remark 4.10. Lemma 4.3 is the only place where the close packing condition is necessary to obtain the desired estimate (4.7) because we needed uniform Lipschitz regularity of triangles $\triangle_{ijk}$.

As a corollary of Lemmas 4.1 and 4.3 we have the main result of this section: the accuracy of approximation of the effective viscous dissipation rate by the dissipation rate of the fictitious fluid given in the following proposition.

Proposition 4.3. *Suppose Ω_F satisfies the close packing condition. Then*

$$|\widehat{W} - \widehat{W}_{\boldsymbol{\Pi}}| \leq \mu \left(\sum_{i\in\mathbb{I}} \sum_{j\in\mathcal{N}_i} C_1 R^2 \widehat{\beta}_{ij}^2 + C_2 |\widehat{\boldsymbol{U}}^i - \widehat{\boldsymbol{U}}^j|^2 + C_3 \sum_{i\in\mathbb{I}\cup\mathbb{B}} R^2 (\widehat{\omega}^i)^2 \right), \tag{4.8}$$

where $(\widehat{\mathbb{U}}, \widehat{\boldsymbol{\omega}}, \widehat{\boldsymbol{\beta}}^*)$ minimizes (4.2).

5 Discrete Network

In the previous chapter we described the discrete network that arises from the fictitious fluid approach. Indeed, the equation (4.2) in view of (4.3) is

$$\widehat{W}_{\boldsymbol{\Pi}} = \min_{(\mathbb{U},\boldsymbol{\omega},\boldsymbol{\beta}^*)\in\boldsymbol{\mathcal{R}}^*} \sum_{i\in\mathbb{I},j\in\mathcal{N}_i} W_{\Pi_{ij}}(\boldsymbol{u}) =: \min_{(\mathbb{U},\boldsymbol{\omega},\boldsymbol{\beta}^*)\in\boldsymbol{\mathcal{R}}^*} \mathcal{W}(\mathbb{U},\boldsymbol{\omega},\boldsymbol{\beta}^*), \tag{5.1}$$

where $\boldsymbol{u}$ is the solution of (4.3) and $\mathcal{W}$ is a positive definite quadratic form of $(\mathbb{U},\boldsymbol{\omega},\boldsymbol{\beta}^*)$.

Our next objective is to find coefficients of $\mathcal{W}$ asymptotically as characteristic distance $\delta\to 0$. We have the following result.

Lemma 5.4. *Suppose $\widehat{W}_{\boldsymbol{\Pi}}$ is defined by* (2.10)*, $\mathcal{I}$ is defined by* (2.34)*, $\mathcal{W}$ is defined by* (5.1)*, and Q is defined by* (2.33)-(2.37)*. Then*

$$|\mathcal{W}(\mathbb{U},\boldsymbol{\omega},\boldsymbol{\beta}^*)-Q(\mathbb{U},\boldsymbol{\omega},\boldsymbol{\beta})| \le \mu\left(\sum_{i\in\mathbb{I}}\sum_{j\in\mathcal{N}_i} C_1R^2\beta_{ij}^2 + C_2|\boldsymbol{U}^i-\boldsymbol{U}^j|^2 + C_3\sum_{i\in\mathbb{I}\cup\mathbb{B}} R^2(\omega^i)^2\right) \tag{5.2}$$

for any $(\mathbb{U},\boldsymbol{\omega},\boldsymbol{\beta^*})\in\boldsymbol{\mathcal{R}}^*$ and β_{ij} related to β_{ij}^* through (2.32)*. In particular,*

$$|\widehat{W}_{\boldsymbol{\Pi}}-\mathcal{I}| \le \mu\left(\sum_{i\in\mathbb{I}}\sum_{j\in\mathcal{N}_i} C_1R^2\widehat{\beta}_{ij}^2 + C_2|\widehat{\boldsymbol{U}}^i-\widehat{\boldsymbol{U}}^j|^2 + C_3\sum_{i\in\mathbb{I}\cup\mathbb{B}} R^2(\widehat{\omega}^i)^2\right). \tag{5.3}$$

where $(\widehat{\mathbb{U}},\widehat{\boldsymbol{\omega}},\widehat{\boldsymbol{\beta}})$ is the minimizer of Q.

This Lemma shows that coefficients of $\mathcal{W}(\mathbb{U},\boldsymbol{\omega},\boldsymbol{\beta}^*)$ tend to infinity as $\delta\to 0$ because the corresponding coefficients of $Q(\mathbb{U},\boldsymbol{\omega},\boldsymbol{\beta})$ are asymptotically large and given in (2.36)-(2.37). As mentioned above, the proof of this lemma can be found Chapter 6 of [10].

Combining Proposition 4.3 and Lemma 5.4 we obtain the claim of Proposition 2.1.

In order to prove Theorems 2.1 and 2.2 it remains to show that the error term of the right hand side of (5.3) becomes relatively small compared to the effective discrete dissipation rate $\mathcal{I}$. In order to show that we prove in the next lemma that $\mathcal{I}\to\infty$ as $\delta\to 0$. More specifically we have the following result.

Lemma 5.5. *Suppose Ω_F satisfies the close packing condition. Then there exists a constant $C>0$ such that for every $\{\boldsymbol{U}^i\}$:*

$$\begin{aligned}\mathcal{I} \ge \mu\sum_{i\in\mathbb{I}}\sum_{j\in\mathcal{N}_i} & C_1\delta^{-3/2}|\boldsymbol{U}^i-\boldsymbol{U}^j|^2 + C_2\delta^{-1/2}R^2(\omega^i+\omega^j)^2 \\ & + C_3\delta^{-1/2}R^2(\omega^i-\omega^j)^2 + C_4\delta^{-5/2}\beta_{ij}^2, \quad as \quad \delta\to 0.\end{aligned} \tag{5.4}$$

For the proof of this lemma see Chapter 5 of [10].

From Lemma 5.5 and Proposition 2.1 we have Theorem 2.2, and Theorem 2.1 follows from Theorem 2.2 and Proposition 4.3.

6 Conclusions

In this paper the asymptotic formula for the effective viscous dissipation rate is obtained, where *all* singular terms are derived and justified. This is done by developing a new technical tool - the two-step fictitious fluid approach. Such approach is expected to be helpful in evaluation of effective properties of various highly packed particulate composites. In contrast to partial analysis of microflows, done in the previous studies of concentrated suspensions, the obtained asymptotics provides for a complete picture of microflows. A new term due to the Poiseuille microflow is obtained. It is shown that this Poiseuille microflow does not contribute to singular behavior of viscous dissipation rate in 3D. While in 2D it may result in an anomalous rate of blow-up (of order $\delta^{-5/2}$). Indeed, such a rate of blow-up is obtained in the presence of external field (e.g. gravity) or due to the boundary layer effects. Also our analysis suggests that in absence of an external field the anomalous blow-up does not occur.

The obtained asymptotics expresses the *continuum* dissipation rate in terms of a *discrete* dissipation rate, and the latter reveals dependence on the key physical parameters.

Our study leads to a somewhat surprising observation that suspensions are actually harder to analyze in 2D than in 3D. As we mentioned above, the Poiseuille type microflow is significant in 2D and it is negligible in 3D. The key reason here is topological: in 2D thin gaps between closely spaced inclusions partition the fluid domain into disconnected regions, which is not the case in 3D. Hence, in 2D permeation of fluid between two inclusions contributes into the singular behavior of the effective viscous dissipation rate.

Finally, we note that 2D mathematical models were often used to analyze qualitative behavior of 3D problems in order to reduce the analytical and computational complexity of the problem. Our work clearly shows limits of validity of such modeling.

A Appendix

Coefficients of the quadratic form Q

Define $r_{ij} = R/d_{ij}$. Then the coefficients $\boldsymbol{\mathcal{C}}_k^{ij}$, $k = 1, \dots, 9$, and $\boldsymbol{\mathcal{B}}_m^{ij}$, $m = 1, \dots, 14$ in (2.36) and (2.37), respectively, are given by

$$
\begin{aligned}
&\boldsymbol{\mathcal{C}}_1^{ij} = \frac{1}{2}\pi\mu r_{ij}^{1/2}, \quad \boldsymbol{\mathcal{C}}_2^{ij} = \frac{3}{4}\pi\mu r_{ij}^{3/2}, \quad \boldsymbol{\mathcal{C}}_3^{ij} = \frac{207}{320}\pi\mu r_{ij}^{1/2},\\
&\boldsymbol{\mathcal{C}}_4^{ij} = \frac{9}{4}\pi\mu r_{ij}^{5/2}, \quad \boldsymbol{\mathcal{C}}_5^{ij} = \frac{99}{160}\pi\mu r_{ij}^{3/2}, \boldsymbol{\mathcal{C}}_6^{ij} = \frac{29241}{17920}\pi\mu r_{ij}^{1/2},\\
&\boldsymbol{\mathcal{C}}_7^{ij} = -3\pi\mu r_{ij}^{3/2}, \boldsymbol{\mathcal{C}}_8^{ij} = \frac{9}{40}\pi\mu r_{ij}^{1/2}, \quad \boldsymbol{\mathcal{C}}_9^{ij} = \frac{3}{2}\pi\mu r_{ij}^{1/2},\\
&\boldsymbol{\mathcal{B}}_1^{ij} = 18\pi\mu r_{ij}^{5/2}, \quad \boldsymbol{\mathcal{B}}_2^{ij} = \frac{51}{20}\pi\mu r_{ij}^{3/2}, \quad \boldsymbol{\mathcal{B}}_3^{ij} = \frac{20889}{2240}\pi\mu r_{ij}^{1/2},\\
&\boldsymbol{\mathcal{B}}_4^{ij} = 4\pi\mu r_{ij}^{1/2}, \quad \boldsymbol{\mathcal{B}}_5^{ij} = \frac{9}{2}\pi\mu r_{ij}^{1/2}, \quad \boldsymbol{\mathcal{B}}_6^{ij} = 6\pi\mu r_{ij}^{3/2},\\
&\boldsymbol{\mathcal{B}}_7^{ij} = \frac{63}{20}\pi\mu r_{ij}^{1/2}, \boldsymbol{\mathcal{B}}_8^{ij} = 6\pi\mu r_{ij}^{3/2}, \quad \boldsymbol{\mathcal{B}}_9^{ij} = \frac{19}{20}\pi\mu r_{ij}^{1/2},\\
&\boldsymbol{\mathcal{B}}_{10}^{ij} = -3\pi\mu r_{ij}^{3/2}, \boldsymbol{\mathcal{B}}_{11}^{ij} = -\frac{3}{8}\pi\mu r_{ij}^{1/2}, \boldsymbol{\mathcal{B}}_{12}^{ij} = -3\pi\mu r_{ij}^{1/2},\\
&\boldsymbol{\mathcal{B}}_{13}^{ij} = -3\pi\mu r_{ij}^{1/2}, \boldsymbol{\mathcal{B}}_{14}^{ij} = 6\pi\mu r_{ij}^{1/2}.
\end{aligned}
\tag{A.1}
$$

References

1. Abbot, J. R., Tetlow, N., Graham, A. L., Altobell, S. A., Fukushima, E., Mondy, L.A. and Stephens, T.A.: Experimental observations of particle migration in concentrated suspensions: Couette flow, *J. Rheol.*, **35**, 1991, pp. 773–95.
2. Acheson, D. J.: *Elementary Fluid Dynamics*, Clarendon Press, 1990.
3. Averbakh, A., Shauly, A., Nir, A. and Semiat, R., Slow viscous flows of highly concentrated suspensions–part I. Laser-Doppler velocitometry in rectangular ducts, *Int. J. Multiphase Flow*, **23**, 1997, pp. 409–424.
4. Averbakh, A., Shauly, A., Nir, A. and Semiat, R., Slow viscous flows of highly concentrated suspensions–part II. Particle migration, velocity and concentration profiles in rectangular ducts, *Int. J. Multiphase Flow*, **23**, 1997, pp. 613–629.
5. Aurenhammer, F., Klein, R.: Voronoi Diagrams. In: Sack J. and Urrutia G. (ed) Handbook of Computational Geometry. Chapter V, 201–290. Elsevier Science Publishing (2000).
6. Batchelor, G.K.: *An introduction to fluid dynamics*, Cambridge University Press, 1967.
7. Berlyand, L., Borcea, L., Panchenko, A.: Network Approximation for Effective Viscosity of Concentrated Suspensions with Complex Geometry, *SIAM Journal on Mathematical Analysis*, **36:5**, 2005, pp. 1580–1628.
8. Berlyand, L., Golovaty, D., Movchan, A., Phillips, J., Transport properties of densely packed composites. Effect of shapes and spacings of inclusions. *Quart. J. Mech. Appl. Math.*, **57:4**, 2004, pp. 495–528.
9. Berlyand, L., Gorb, Y. and Novikov A.: Discrete Network Approximation for Highly-Packed Composites with Irregular Geometry in Three Dimensions, in *Multiscale Methods in Science and Engineering*, B. Engquist, P. Lotstedt, O. Runborg, eds., *Lecture Notes in Computational Science and Engineering* **44**, Springer, 2005, pp. 21-58.
10. Berlyand, L., Gorb, Y. and Novikov A.: Fictitious Fluid Approach and Anomalous Blow-up of the Dissipation Rate in a 2D Model of Concentrated Suspensions. Preprint available at `http://arxiv.org/abs/math/0608671`.

11. Berlyand, L., Kolpakov, A.: Network Approximation in the Limit of Small Interparticle Distance of the Effective Properties of a High Contrast Random Dispersed Composite, *Arch. Rat. Math. Anal.*, **159:3**, 2001, pp. 179–227.
12. Berlyand, L., Novikov, A.: Error of the Network Approximation for Densely Packed Composites with Irregular Geometry, *SIAM J. Math. Anal.*, **34:2**, 2002, pp. 385–408.
13. Berlyand, L., and Panchenko, A.: Strong and weak blow up of the viscous dissipation rates for concentrated suspensions, *J. Fluid Mech.*, **578**, 2007, pp. 1–34.
14. Borcea, L.: Asymptotic analysis of quasi-static transport in high contrast conductive media. *SIAM J. Appl. Math.*, **59:2**, pp. 597–635.
15. Borcea, L., Berryman, J.G., Papanicolaou, G.C.: Matching pursuit for imaging high-contrast conductivity. *Inverse Problems*, **15**, 1999, pp. 811–849.
16. Borcea, L., and Papanicolaou, G.: Network approximation for transport properties of high contrast materials, *SIAM J. Appl. Math.*, **58:2**, 1998, pp. 501–539.
17. Brady, J.F. and Bossis, G., The rheology of concentrated suspensions of spheres in simple shear flow by numerical simulation, *J. Fluid Mech.*, **155**, 1985, pp. 105–129.
18. Brenner, S. C.: Korn's inequalities for Piecewise H^1 Vector Fields, *Mathematics of Computation*, **73:247**, 2003, pp. 1067–1087.
19. Bürger, R. and Wendland, W. L.: Sedimentation and suspension flows: historical perspective and some recent developments. Sedimentation and suspension flows: some recent contributions (Stuttgart, 1999). *J. Engrg. Math.*, **41:2-3**, 2001, pp. 101–116.
20. Camargo, M. and Tellez, G., Renormalized charge in a two-dimensional model of colloidal suspension from hypernetted chain approach, preprint accessible at http://aps.arxiv.org/pdf/cond-mat/0702056.
21. Chow, A. W., Sinton, S. W. and Iwamiya, J. H. Shear-induced particle migration in Couette and parallel plate viscosmeters: NMR imaging and stress measurements, *Phys. Fluids A*, **6**, 1994, pp. 2561–2575.
22. Czuchaj, E., Rebentrost, F., Stoll, H., Preuss, H., Ingco, S.P., Miskin, I., Elliott, L., Ingham, D.B. and Hammond, P.S., Steady suspension flows into two-dimensional horizontal and inclined channels, *International Journal of Multiphase Flow*, **22:6**, 1996, pp. 1223–1246.
23. Ding, J., Warriner, H. E. and Zasadzinski J. A.: Viscosity of Two-Dimensional Suspensions, *Phys. Rev. Lett.*, **88:16**, 2002.
24. Einstein, A.: Eine neue Bestimmung der Moleküuldimensionen, *Ann.Phys.*, **19**, 1906, p. 289, and **34**, 1906, p. 591.
25. Ekeland, I. and Temam, R. *Convex Analysis and Variational Problems*, North-Holland Pub. Co., 1976.
26. Frankel, N. A. and Akrivos, A., On the viscosity of a concentrated suspensions of solid spheres, *Chemical Engineering Science*, **22**, 1967, pp. 847–853.
27. Friesecke, G. and Theil, F., Validity and failure of the Cauchy-Born hypothesis in a two-dimensional mass-spring lattice. *J. Nonlinear Sci.*, **12:5**, 2002, pp. 445–478.
28. Galdi, G.P. *An introduction to the mathematical theory of the Navier-Stokes equations*, Vol. I, 1994.
29. Graham A. L.: On the Viscosity of Suspensions of Solid Spheres, Report RRC 62, Rheology Research Center, the University of Wisconsin, June 1980.
30. Gustavsson, K., *Mathematical and Numerical Modeling of 1-D and 2-D Consolidation*, Doctoral Dissertation, Royal Institute of Technology, 2003.

31. Gustavson, K. and Oppelstrup, J.: Numerical 2D models of consolidation of dense flocculated suspensions, *J. of Eng. Math.*, **41:2/3**, 2001, pp. 189–201.
32. Gustavsson, K., Oppelstrup, J. and Eiken, J.: Consolidation of concentrated suspensions - shear and irreversible floc structure rearrangements, Computing and Visualization in Science, **4**, 2001, pp. 61–66.
33. Hadj-Rabia, N., Mekbel, S. and Bouhadef, M., On solid transport in suspension in a waterway: a two dimensional numerical approach, *Computer Methods in Water Resources*, **12:2**, 1998.
34. Hampton, R. E., Mammoli, A. A., Graham, A. L. and Tetlow, N., Migration of particles undergoing pressure-driven flow in a circular conduit, *J. Rheol.*, **41**, 1997, pp. 621–640.
35. Hasimoto, H., On the periodic fundamental solutions of the Stokes' equations and their application to viscous flow past a cubic array of spheres, *J. Fluid Mech.*, **5**, 1959, pp. 317–328.
36. Hestenes, Magnus R.: *Optimization Theory. The Finite Dimensional Case*, John Wiley & Sons, New York/London/Sidney/Toronto, 1975.
37. Hoekstra, H., Vermant, J., Mewis, J. and Fuller, G. G.: Flow-Induced Anisotropy and Reversible Aggregation in Two-Dimensional Suspensions, *Langmuir*, **19:22**, 2003.
38. Juárez L. H., Glowinski R. and Pan T. W., Numerical simulation of the sedimentation of rigid bodies in an incompressible viscous fluid by Lagrange multiplier/fictitious domain methods combined with the Taylor-Hood finite element approximation. Proceedings of the Fifth International Conference on Spectral and High Order Methods (ICOSAHOM-01) (Uppsala), *J. Sci. Comput.*, **17:1-4**, 2002, pp. 683–694.
39. Keller, J. B.: Conductivity of a Medium Containing a Dense Array of Perfectly Conducting Spheres or Cylinders or Nonconducting Cylinders, *J. Appl. Phys.*, **34:4**, 1963, pp. 991–993.
40. Koh, C., Leal, L. G. and Hookham, P. A., An experimental investigation of concentrated suspension flow in a rectangular channel, *J. Fluid Mech.*, **256**, 1994, pp. 1–32.
41. Kozlov, S. M.: Geometrical aspects of averaging, *Russ. Math. Surveys*, **44:22**, 1989, pp. 91–144.
42. Ladd, A. J. C., Sedimentation of homogeneous suspensions of non-Brownian spheres, Phys. Fluids, **9:3**, 1997, pp. 491–499.
43. Ladyzhenskaya, O. A. and Ural'tseva, N. N.: *Linear and Quasilinear Elliptic Equations*, Academic press, New York/London, 1968.
44. Landau, L. D. and Lifshits, E. M. *Fluid mechanics*, Pergamon Press, 1987.
45. Leal, L. G. *Laminar Flow and Convective Transport Processes: Scaling Principles and Asymptotic Analysis*, Butterworth-Heinemann, 1992.
46. Leighton, D. and Acrivos, A., Measurement of shear-induced self-diffusion in concentrated suspensions of spheres, *J. Fluid Mech.*, **177**, 1987, pp. 109–131.
47. Lyon, M. and Leal, L. G., An Experimental Study of the Motion of Concentrated Suspensions in Two-Dimensional Channel Flow. I. Monodisperse Systems, *J. Fluid Mech.*, **363**, 1998, pp. 25–56.
48. Lyon, M. and Leal, L. G., An Experimental Study of the Motion of Concentrated Suspensions in Two-Dimensional Channel Flow. II. Bidisperse Systems, *J. Fluid Mech.*, **363**, 1998, pp. 57–77.
49. Maury, B., Direct simulations of 2D fluid-particle flows in biperiodic domains, *J. Comput. Phys.*, **156:2**, 1999, pp. 325–335.

50. Newman, M. E. J.: The Structure and Functions of Complex Networks, *SIAM Review*, **45:2**, 2003, pp. 167–256.
51. Nott, P. R. and Brady, J. F., Pressure-driven flow of suspensions: simulation and theory, *J. Fluid Mech.*, **275**, 1994, pp. 157–199.
52. Nunan, K. C. and Keller, J. B.: Effective viscosity of a periodic suspension, *J. Fluid Mech.*, **142**, 1984, pp. 269–287.
53. Pasquero, C., Provenzale, A. and Spiegel, E.A., Suspension and Fall of Heavy Particles in Random Two-Dimensional Flow, *Physical Review Letters*, **91:5**,2003, pp.054502(4).
54. Phillips, R. J., Armstrong, R. C., Brown, R. A., Graham, A. L. and Abbot, J. R., A constitutive equation for concentrated suspensions that accounts for shear-induced particle migration, *Phys. Fluids A*, **4**, 1992, pp. 30–40.
55. Records, A. and Sutherland, K., *Decanter Centrifuge Handbook*, Elsevier, 2001.
56. Sierou, A. and Brady, J. F.: Accelerated Stokesian dynamic simulations, *J. Fluid Mech.*, **448**, 2001, pp. 115–146.
57. Sokolov, A., Aranson, I. S., Kessler, J. O. and Goldstein, R. E.: Concentration Dependence of the Collective Dynamics of Swimming Bacteria, *Phys. Rev. Let.*, **98:15**, 2007, pp. 158102-1–4.
58. Subia, S, Ingber, M. S., Mondy, L. A., Altobelli, S. A. and Graham, A. L., Modelling of concentrated suspensions using a continuum constitutive equation, *J. Fluid Mech.*, **373**(1998), 193–219.
59. Temam, R. *Navier-Stokes equations: theory and numerical analysis*, AMS Chelsea Pub., 2001.
60. Wilson, H. J. and Davis, R. H., The effect of different particle contacts on suspension rheology, *XXI ICTAM*, 1521 August 2004, Warsaw, Poland.
61. Wu, X.-L. and Libchaber, A., Particle Diffusion in a Quasi-Two-Dimensional Bacterial Bath, *Phys. Rev. Let.*, **84:14**, 2000, pp. 3017–3020.